

doi: 10.12029/gc20210314

周琨,田亚洲,杨经绥,杨华燊,田云雷,武勇,钱丰,许秋媛. 2021. 黔南罗甸酸性岩脉年代学、地球化学及其对火成岩省岩浆活动的响应[J]. 中国地质, 48(3): 854–871.

Zhou Kun, Tian Yazhou, Yang Jingsui, Yang Huashen, Tian Yunlei, Wu Yong, Qian Feng, Xu Qiuyuan. 2021. Geochronology and geochemistry of Luodian acidic dykes in the Southern Guizhou Province and its response to magmatism of igneous province[J]. Geology in China, 48(3): 854–871 (in Chinese with English abstract).

黔南罗甸酸性岩脉年代学、地球化学及其对火成岩省岩浆活动的响应

周琨^{1,2}, 田亚洲^{1,2}, 杨经绥^{3,4}, 杨华燊^{1,2}, 田云雷^{1,2}, 武勇⁵, 钱丰^{1,2}, 许秋媛^{1,2}

(1. 贵州大学资源与环境工程学院, 贵州 贵阳 550025; 2. 贵州大学喀斯特地质资源与环境教育部重点实验室, 贵州 贵阳 550025; 3. 南京大学地球科学与工程学院, 江苏 南京 210023; 4. 中国地质科学院地质研究所 自然资源部深地动力学重点实验室地幔研究中心, 北京 100037; 5. 中核集团核工业北京地质研究院 钫资源勘查与评价技术重点实验室, 北京 100029)

提要:黔南罗甸地区位于峨眉山大火成岩省分布区外带, 区内出露众多与峨眉山玄武岩同期的辉绿岩墙。酸性岩脉为石英二长斑岩, 侵入于辉绿岩中, 对该岩脉的研究有助于丰富峨眉山大火成岩省岩石组合规律及岩浆活动的认识。本文对罗甸酸性岩脉进行了岩石学、SIMS年代学和地球化学研究。岩石主量元素平均含量 SiO₂ 66.83%, CaO 1.76%, Al₂O₃ 14.74%, MgO 0.76%, TFe₂O₃ 4.49%, K₂O 3.67%, Na₂O 5.24%, A/CNK 平均为 0.93, 显示高硅富碱、准铝质的特征。 $(La/Yb)_N=7.71\sim10.60$, 轻重稀土元素分馏强烈, 稀土元素球粒陨石标准化配分曲线呈右倾型, 具有 OIB 特征。 $\delta^{143}\text{Eu}$ 值平均为 0.91, 富集 Rb、Ba、Th、K、Nd 等元素, 强烈亏损 Nb、Ta、P、Ti 等元素。石英二长斑岩($^{87}\text{Sr}/^{86}\text{Sr}$) 和 $\varepsilon_{\text{Nd}}(t)$ 值分别为 0.704247~0.705292、1.08~1.54, 与辉绿岩相似。研究表明, 石英二长斑岩是由地幔柱部分熔融产生的玄武质岩浆经历分离结晶的产物, 并混染了少量上地壳物质。锆石 SIMS U-Pb 年代学研究显示石英二长斑岩年龄为 (259 ± 2) Ma, 与峨眉山大火成岩省岩浆作用时间一致。样品中存在大量继承锆石, 可能为扬子地块不同阶段构造活动的响应。

关 键 词:石英二长斑岩; 岩石地球化学; SIMS 年代学; 峨眉山大火成岩省; 黔南; 地质调查工程

中图分类号:P597; P588.12⁺¹ **文献标志码:**A **文章编号:**1000-3657(2021)03-0854-18

Geochronology and geochemistry of Luodian acidic dykes in the Southern Guizhou Province and its response to magmatism of igneous province

ZHOU Kun^{1,2}, TIAN Yazhou^{1,2}, YANG Jingsui^{3,4}, YANG Huashen^{1,2}, TIAN Yunlei^{1,2}, WU Yong⁵, QIAN Feng^{1,2}, XU Qiuyuan^{1,2}

(1. College of Resources and Environmental Engineering, Guizhou University, Guiyang 550025, Guizhou, China; 2. Key Laboratory of Karst Georesources and Environment, Ministry of Education, Guizhou University, Guiyang 500025, Guizhou, China; 3. School of Earth Sciences and Engineering, Nanjing University, Nanjing 210023, Jiangsu, China; 4. Center for Advanced Research on Mantle

收稿日期:2021-03-12; 改回日期:2021-04-20

基金项目:国家自然科学基金项目(41663005)、贵州大学人才引进项目(702400163301)和贵州省人才基地项目(RCJD2018-12)联合资助。

作者简介:周琨,男,1998年生,硕士生,矿物学、岩石学、矿床学专业;E-mail:zk.gzu@foxmail.com。

通讯作者:田亚洲,男,1987年生,副教授,从事基性、超基性岩岩石学研究;E-mail:tianyazhou87@163.com。

(CARMA), Key Laboratory of Deep-Earth Dynamics of Ministry of Natural Resources, Institute of Geology, Chinese Academy of Geological Sciences, Beijing 100037, China; 5. CNNC Key Laboratory of Uranium Resources Exploration and Evaluation Technology, Beijing Research Institute of Uranium Geology, Beijing 100029, China)

Abstract: Luodian, located in the southern Guizhou Province, belongs to the outer zone of Emeishan Large Igneous Province. Numerous diabase of the same period as the Emeishan Large Igneous Province are exposed in the area. The acidic dykes are quartz monzonite porphyry, and invade into diabase. The study of acidic dykes is conducive to enriching the understanding of the law of lithology combination and magmatism in Emeishan Large Igneous Province. Petrology, SIMS chronological and geochemical studies of the acidic rock in Luodian were performed. Average content of major oxides are SiO₂ 66.83%, CaO 1.76%, Al₂O₃ 14.74%, MgO 0.76%, TFe₂O₃ 4.49%, K₂O 3.67%, Na₂O 5.24%, and average value of A/CNK is 0.93, displaying the features of high silicon, rich alkali and quasi-aluminous. (La/Yb)_N ratios of 7.71 to 10.60 displays apparent differentiation between LREE and HREE with an average δ Eu of 0.91. The chondrite-normalized curve of REE is right inclined, showing ocean island basalts (OIB) signature. The dykes are enriched in elements such as Rb, Ba, Th, K and Nd, and depleted in elements such as Nb, Ta, P and Ti. The values of (⁸⁷Sr/⁸⁶Sr)_i (0.704247–0.705292) and $\varepsilon_{\text{Nd}}(t)$ (1.08–1.54) are similar to those of diabase. It is suggested that the acidic rock is originated from fractional crystallization of basaltic magma produced by partial melting of mantle plume, and contaminated with a small amount of upper crust material. The acidic rock was dated at (259±2)Ma by SIMS, which is consistent with the magmatism age of the Emeishan Large Igneous Province. The large number of inherited zircons in the samples were found, might be the response to tectonic activity at different stages in the Yangtze block.

Key words: quartz monzonite porphyry; petrogeochemistry; SIMS Chronology; ELIP; Southern Guizhou; geological survey engineering

About the first author: ZHOU Kun, male, born in 1998, master candidate, engaged in the research of mineralogy, petrology and deposit; E-mail: zk.gzu@foxmail.com.

About the corresponding author: TIAN Yazhou, male, born in 1987, associate professor, engaged in the research of basic and ultrabasic rocks; E-mail: tianyazhou87@163.com.

Fund support: Funded by National Natural Science Foundation of China (No.41663005), Talent Introduction Projects of Guizhou University (No. 702400163301) and Talent Base Projects of Guizhou Province (No. RCJD2018–12).

1 引言

大火成岩省是指在短时间内巨量喷发溢流玄武岩及伴生的侵入岩所构成的岩浆建造(Ernst et al., 2005)。位于扬子地块西部的峨眉山大火成岩省(Emeishan Large Igneous Province, ELIP)被认为是深部地幔柱岩浆活动的产物(Chung et al., 1998; Xu et al., 2001; Zhou et al., 2002; Ali et al., 2002, 2005; He et al., 2003; Zhang et al., 2006; Song et al., 2008)。ELIP除大规模的溢流玄武岩外,还伴生基性-超基性岩体和少量中酸性岩体。对于ELIP中溢流玄武岩以及基性-超基性岩体的研究,前人取得了丰硕的成果(张招崇等,2001,2005; Xu et al., 2001; Ali et al., 2002; Zhou et al., 2002, 2005; Xiao et al., 2003; He et al., 2010; 李宏博等,2010,2015; Zhong et al., 2011; 徐义刚等,2013)。大火成岩省通常伴随有中酸性岩类出露,与基性岩类呈现出双峰

式的岩石组合特征(Bryan et al., 2008),甚至存在主要由中酸性火成岩组成的大火成岩省(Bryan et al., 2000, 2010)。在ELIP分布范围内,对中酸性岩体的研究主要集中于内带喷发中心区域(罗震宇等,2006;邵辉等,2007; Shellnutt et al., 2007, 2010; Xu et al., 2008; Zhou et al., 2008; 骆文娟等,2011; 李宏博等,2015)。而随着对ELIP中酸性岩体的研究的深入,对中酸性岩体的成因机制方面的认识主要有:镁铁质岩浆结晶分异作用、地壳熔融或幔源岩浆与地壳相互作用、同化与分异结晶作用(Zhong et al., 2007, 2011; 章清文等,2015)等。在贵州境内,峨眉山玄武岩主要分布于西部地区,在南部则以次火山岩相辉绿岩墙的形式出露(贵州省地质矿产局,1987),形成时代为263~255 Ma(韩伟等,2009; 曾广乾等,2014; 张晓静等,2014; 祝明金等,2018),与ELIP喷发时间(259.1~259.2 Ma, Zhong et al., 2014)一致。罗甸地区位于ELIP分布区外带,此次研究的

对象石英二长斑岩侵入于辉绿岩之中,目前对于该岩脉的研究还较有限。因此,本文对黔南罗甸中酸性岩开展了岩石学、SIMS年代学及地球化学方面的研究,确定该岩脉的年龄,探讨其成因以及与ELIP之间的联系。

2 地质背景

研究区位于峨眉山玄武岩分布的外带,地处扬子地块西南缘与右江褶皱带交界地带(图1a)。区内发育北西向紫云—罗甸—南丹断裂和北东向桑郎—罗甸断裂,两条断裂带在罗甸一带交汇。紫云—罗甸—南丹断裂带由上扬子地块南部北西向的裂陷槽演化

而来,该裂陷槽盆自早泥盆世开始进入强烈的构造活动,中泥盆世受到拉伸减薄作用,至二叠世形成了北西向展布的槽盆,控制了泥盆纪至二叠纪的沉积环境、构造形态及两侧台地的岩相分界,为岩浆的侵位活动提供了有利条件(王尚彦等,2005,2006)。研究区和邻区出露众多的辉绿岩墙,在空间上构成了一定规模的岩墙群,反映了伸展拉张的构造背景(韩伟,2010)。区内发育有较多的北西、北东向断层,各类断层、褶皱叠加明显,构造形态复杂。区内出露泥盆系、石炭系、二叠系、三叠系(图1b),其岩性特征详见表1。采样区域的火成岩种类有限,大部分为侵入于二叠系茅口组和栖霞组地层间的辉绿岩,其次为侵入辉

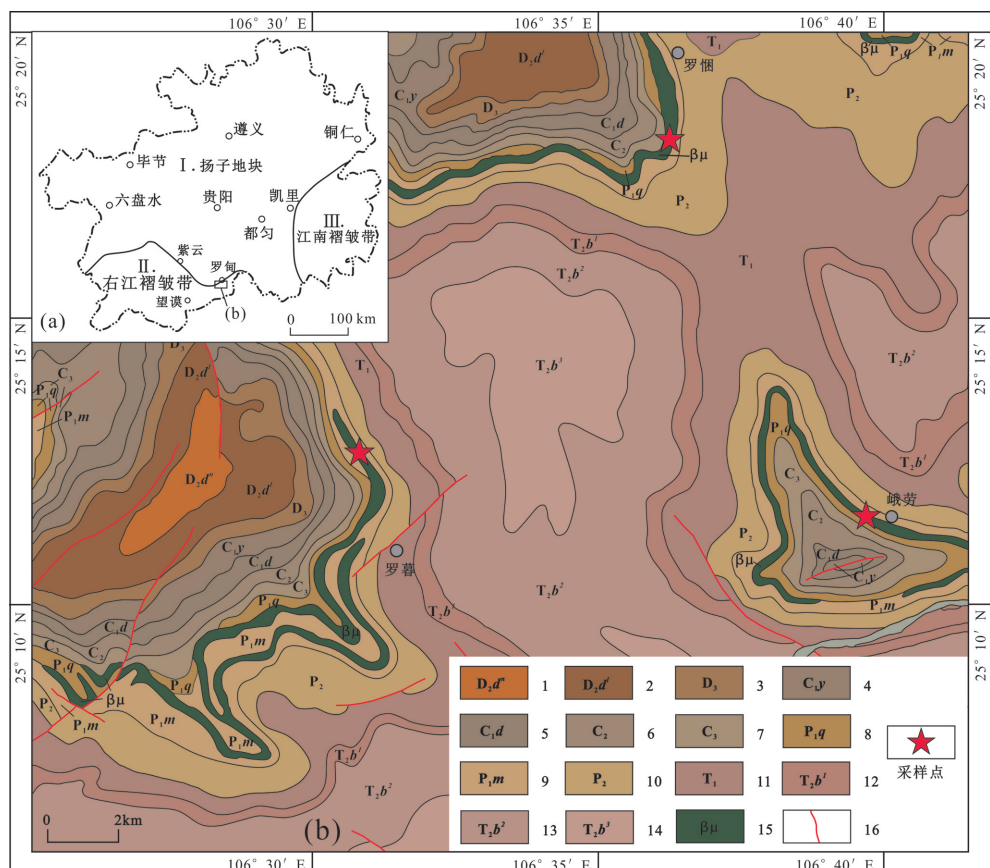


图1 研究区大地构造位置图及地质简图

(a据郝家树等,2014;b据广西壮族自治区地质局,1972修改)

1—东岗岭阶纳标段;2—东岗岭阶罗富段;3—上泥盆统;4—石炭系岩关组;5—石炭系大塘阶;6—中石炭统;7—上石炭统;8—二叠系栖霞组;9—二叠系茅口组;10—上二叠统;11—下三叠统;12—板纳组下段;13—板纳组中段;14—板纳组上段;15—辉绿岩脉;16—断层

Fig.1 Simplified tectonic map showing the location and geological map of the research area

(a, after Hao Jiaxu et al., 2014; b, modified from Guangxi Zhuang Autonomous Region Geology Bureau, 1972)

1—Nabiao Member of Donggangling Stage; 2—Luofu Member of Donggangling Stage; 3—Upper Devonian; 4—Yanguan Formation of Carboniferous; 5—Datang Formation of Carboniferous; 6—Middle Carboniferous; 7—Upper Carboniferous; 8—Qixia Formation of Permian; 9—Maokou Formation of Permian; 10—Upper Permian; 11—Lower Triassic; 12—Lower Member of Banna Formation; 13—Middle Member of Banna Formation; 14—Upper Member of Banna Formation; 15—Diabase dykes; 16—Fault

表 1 研究区出露地层岩性特征
Table 1 Lithology of outcropped strata in the research area

地 层		岩 性 特 征 描 述
泥盆系(D)	中统(D ₂)	①东岗岭阶纳标段(D _{2d'}):深灰、黑色薄层状页岩夹粉沙质页岩; ②东岗岭阶罗富段(D _{2d'}):深灰、黑色薄—中层状钙质页岩和页岩夹泥质灰岩(或互层)
	上统(D ₃)	浅灰、灰白色中—厚层鲕状、假鲕状灰岩及灰岩
	下统(C ₁)	①岩关组(C _{1y}):灰、深灰色薄—中层状灰岩,下部夹泥质灰岩,或薄层状硅质岩、硅质页岩夹粉砂质页岩和泥质灰岩; ②大塘组(C _{1d}):浅灰色中—厚层状灰岩或深灰色燧石灰岩夹硅质岩、页岩灰、灰黑色燧石灰岩夹少许硅质岩,下部夹白云质灰岩
石炭系(C)	中统(C ₂)	浅灰色灰岩夹少许白云质灰岩或深灰色燧石灰岩夹硅质岩、页岩
	上统(C ₃)	①栖霞组(P _{1q}):浅灰、深灰色灰岩,底部灰岩含泥质。或深灰色、黑色燧石灰岩夹硅质岩,底部具8~20 m厚的钙质页岩、泥质粉砂岩或硅质岩; ②茅口组(P _{1m}):灰、浅灰色中厚层状灰岩夹白云质灰岩。或深灰色、黑色燧石灰岩夹硅质岩,顶部夹角砾状灰岩
	下统(P ₁)	灰绿色层状火山碎屑岩、硅质岩、硅质页岩及燧石页岩,底部夹锰土层
二叠系(P)	上统(P ₂)	上部为泥质扁豆状灰岩、泥质灰岩,下部页岩夹少量粉砂质页岩,底部夹薄层灰岩。或上部为泥灰岩夹页岩,下部页岩夹粉砂质页岩、少量硅质岩和硅质页岩
	下统(T ₁)	①板纳组下段(T _{1b'}):青灰、灰绿色薄层状粉砂质页岩、粉砂岩,底部夹火山碎屑岩; ②板纳组中段(T _{1b'}):上部为青灰、灰绿色页岩夹粉砂岩。中部为灰绿色中—厚层状或块状细砂岩夹粉砂岩及页岩(厚44~50 m)。底部为青灰色中—厚层状细砂岩夹页岩(厚60~75 m); ③板纳组上段(T _{1b''}):上部及中部为青灰色页岩、钙质页岩、泥质灰岩、灰岩夹粉砂岩。底部为灰绿色厚层块状钙质细砂岩夹页岩及少许长石石英细砂岩(厚137~160 m)
	中统(T ₂)	

注:据资料^①整理。

绿岩内的石英二长斑岩脉。

3 岩脉出露概况和样品特征

罗悃采样点位于罗甸县罗悃镇以南1 km,地理坐标为25°18'50"N, 106°36'13"E。该点出露的石英二长斑岩脉宽50 cm,产状近于直立(图2a),岩石中可见大量针状长石颗粒,长石颗粒大小多集中在0.5 mm,偶见矿物颗粒大于1 mm。石英二长斑岩侵入于风化较严重的辉绿岩中,可见辉绿岩被包裹在石英二长斑岩内部(图2b)。

峨劳采样点位于罗甸县峨劳村以东约1 km处,地理坐标为25°12'14"N, 106°40'14"E。该点上覆地层为灰岩,在地貌上表现为悬崖,底部为辉绿岩岩墙,两者之间的地层界限明显。辉绿岩风化严重,可见球状风化辉绿岩。石英二长斑岩脉穿插于辉绿岩岩墙中,宽度大小不一,较大者宽约2 m,较小

者宽10~20 cm(图2c~d)。

罗暮采样点位于罗甸县罗暮乡玉石场,地理坐标为25°12'35"N, 106°31'11"E。该点出露的辉绿岩风化严重,几乎风化成土状,部分辉绿岩风化成球状,球形中辉绿岩较为新鲜。可见少量穿插侵入的石英二长斑岩,侵入方向杂乱(图2e)。

采集的岩石均无明显蚀变,为块状构造,在显微镜下呈斑状结构,斑晶主要为斜长石、钾长石和石英,基质主要为斜长石、石英、黑云母和副矿物(图3)。斜长石呈板状、长条状,发育聚片双晶,具弱钠黝帘石化,蚀变后表面混浊,粒径0.2~2 mm,含量45%~55%。钾长石长条状或粒状,发育卡式双晶,粒径0.2~1 mm,含量15%~20%。石英呈他形,粒径0.1~0.2 mm,含量10%~15%。黑云母呈残片状分布于斜长石和钾长石之间,含量约5%。角闪石含量很少(<3%)。观察到少量不透明副矿物,矿物



图 2 罗甸酸性岩脉露头

a—罗甸石英二长斑岩露头;b—辉绿岩被包裹在石英二长斑岩内;c、d—峨劳石英二长斑岩露头;e—罗甸石英二长斑岩露头

Fig.2 Outcrop of acidic dyke in Luodian

a—Outcrop of quartz monzonite porphyry in Luokun; b—Diabase is enclosed in quartz monzonite porphyry; c,d—Outcrop of quartz monzonite porphyry in Elao; e—Outcrop of quartz monzonite porphyry in Luomu

成分为磁铁矿,含量约2%。

4 分析测试方法

样品全岩主量元素、微量元素和稀土元素分析在广州澳实分析检测有限公司完成,主量元素采用熔片X-射线荧光光谱法(P61-XRF26S)测定,并通过等离子光谱与化学法测定进行互相检测,稀土、

微量元素元素采用熔片和酸溶等离子质谱法(M61-MS81)测定。

锆石U-Th-Pb同位素分析在中核集团核工业北京地质研究院分析测试研究所的Cameca SIMS 1280 HR型二次离子质谱仪上进行。U、Th、Pb同位素比值用标准锆石Plešovice校正获得(Sláma et al., 2008)。U、Th浓度用标准锆石91500校正获得,实

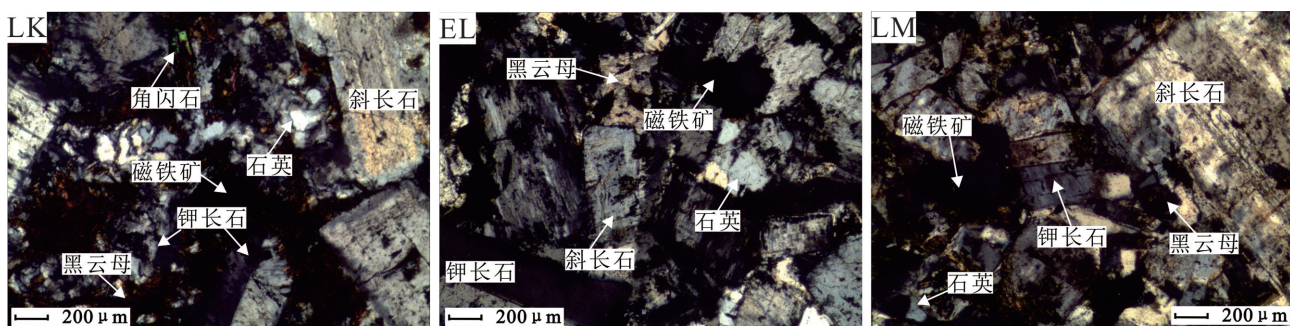


图 3 石英二长斑岩正交偏光显微照片

LK—罗甸样品;EL—峨劳样品;LM—罗甸样品

Fig. 3 Microphotographs of the quartz monzonite porphyry (crossed nicols)

LK—Samples of Luokun; EL—Samples of Elao; LM—Samples of Luomu

验流程和数据处理详见(Li et al., 2009)。普通Pb校正采用实测²⁰⁴Pb值。由于测得的普通Pb含量非常低,假定普通Pb主要来源于制样过程中带入的表面Pb污染,因此用现代地壳的平均Pb同位素组成作为普通Pb组成进行校正(Stacey et al., 1975)。单点分析的同位素比值及年龄误差均为 1σ 。数据处理采用Isoplot软件(Ludwig, 2003)。

Sr-Nd同位素测试在贵州同微科技有限公司超净实验室内完成,Sr、Nd同位素比值的质量分馏校正分别基于⁸⁶Sr/⁸⁸Sr=0.1194和¹⁴³Nd/¹⁴⁴Nd=0.7219。Sr同位素测试使用VG Sector 54 TIMS仪器进行,测定Sr同位素标样NBS987的⁸⁷Sr/⁸⁶Sr值为0.710222 $\pm 20(2\sigma)$;Nd同位素比值测定在Nu Plasma HR MC-ICP-MS仪器上完成,测定Nd同位素标样Ames的¹⁴³Nd/¹⁴⁴Nd值为0.511966 $\pm 16(2\sigma)$ 。

5 分析结果

5.1 主量元素特征

主量元素结果见表2。样品SiO₂含量为63.94%~70.53%(平均为66.83%);K₂O含量为1.99%~5.34%(平均为3.67%);Na₂O含量为4.35%~5.89%(平均为5.24%);(Na₂O+K₂O)为7.58%~10.39%,Na₂O/K₂O为0.95~2.96,显示其富碱的特征;Al₂O₃含量为12.88%~15.98%(平均为14.74%)。数据处理时,去除烧失量,对各主量元素归一化至100%后重新计算。里特曼指数 σ 值介于2.07~4.61(平均为

3.37);铝饱和指数A/CNK为0.86~0.97(平均为0.93),分异指数(DI)为82.27~88.42。在(Na₂O+K₂O)-SiO₂分类图中,来自罗甸和峨劳的样品落入石英二长岩区域内,而来自罗暮的样品落入花岗闪长岩和花岗岩交界区域(图4);在A/NK-A/CNK图解中所有样品均落入准铝质区域(图5a);在SiO₂-K₂O分类图上,除1个罗暮样品属钙碱性岩石,多数样品落在高钾钙碱性范围内(图5b),而来自罗甸的样本数据均落入钾玄岩系列范围内,显示该岩脉富钾的特征。

5.2 稀土及微量元素特征

稀土与微量元素结果见表2。样品ΣREE为 331.32×10^{-6} ~ 452.58×10^{-6} ,稀土含量总体较高;LREE/HREE=8.03~9.59,(La/Yb)_N=7.71~10.60,轻重稀土分馏强烈, δ Eu值为0.77~1.05(平均为0.91),表现出弱的Eu负异常。在球粒陨石标准化稀土元素配分图(图6a)中,样品呈现出右倾型分配曲线,与OIB相似。在原始地幔标准化微量元素蛛网图(图6b)中,明显富集Rb、Ba、Th、K、Nd等元素,强烈亏损Nb、Ta、P、Ti等元素。

5.3 锆石SIMS U-Pb定年结果

每个采样点分别选取20颗锆石进行SIMS U-Pb同位素年龄测试。在筛选和处理分析结果的过程中,按一定规则舍去部分不适用的数据,具体规则如下:分析区域混入了包体或其他杂质的点;单点年龄分析偏差较大的点;²⁰⁶Pb/²⁰⁴Pb<1000的点(Heaman et al., 1993; Wingate et al., 2000; Li et al., 2010)。

锆石SIMS U-Pb定年结果见表图7和表3。样品中的锆石晶形较完整,为柱状、粒状的自形一半自形锆石,短轴长度为50~100 μm,长轴长度约50~150 μm。LM样品中的锆石磨圆度差,为棱角状,CL图像普遍较暗,缺失岩浆振荡环带结构,暗示石英二长斑岩原始岩浆的成分均一,经历了比较快速的侵位过程;EL样品中的锆石磨圆度较好,CL图像显示多数锆石核部具有清晰的振荡环带结构,边部则有亮白色的增生边存在;LK样品中的锆石CL图像显示其外形为次棱角状,具有清晰的岩浆振荡环带结构。年龄>1000 Ma的锆石使用²⁰⁷Pb/²⁰⁶Pb年龄,<1000 Ma的锆石使用²⁰⁶Pb/²³⁸U年龄。LK样品中锆石年龄较为分散,除LK-13和LK-5测

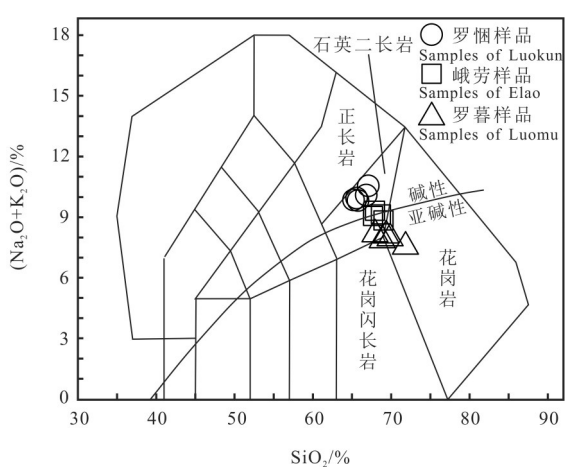


图4 (Na₂O+K₂O)-SiO₂图(据Middlemost, 1994)
Fig.4 (Na₂O+K₂O)-SiO₂ diagram (after Middlemost, 1994)

表 2 主量元素(%)、微量及稀土元素(10^6)分析结果
Table 2 Analytical results major elements (%), trace elements and REEs (10^6)

测试 项目	样 号													
	LK1	LK2	LK3	LK4	LK5	EL1	EL2	EL3	EL4	LM1	LM2	LM3	LM4	LM5
SiO ₂	65.01	63.94	64.41	66.12	65.68	67.70	67.71	66.62	67.10	68.42	70.53	66.57	68.27	67.49
TiO ₂	0.80	0.77	0.76	0.60	0.72	0.65	0.54	0.65	0.65	0.51	0.41	0.54	0.47	0.50
Al ₂ O ₃	15.32	15.40	15.20	15.98	15.34	15.20	14.85	15.55	15.04	13.74	12.88	14.10	13.57	14.21
TFe ₂ O ₃	5.42	5.64	5.45	3.38	4.38	3.65	3.79	3.97	4.03	4.83	4.04	5.19	4.51	4.52
MnO	0.14	0.12	0.12	0.10	0.12	0.04	0.04	0.05	0.06	0.05	0.04	0.05	0.05	0.05
MgO	0.85	0.89	0.90	0.47	0.62	0.52	0.68	0.67	1.16	0.89	0.67	0.87	0.71	0.73
CaO	1.39	1.44	1.42	1.43	1.38	1.68	1.73	1.84	1.40	1.98	1.98	2.37	2.11	2.54
Na ₂ O	5.35	5.41	5.48	5.05	5.00	5.79	4.96	5.79	5.37	4.92	4.35	5.12	4.87	5.89
K ₂ O	4.35	4.24	4.28	5.34	4.89	3.20	3.70	3.09	3.82	3.24	3.23	2.99	3.08	1.99
P ₂ O ₅	0.20	0.19	0.18	0.09	0.14	0.10	0.08	0.11	0.11	0.08	0.06	0.11	0.08	0.08
LOI	1.52	1.41	1.22	1.10	1.35	1.06	1.45	1.57	1.22	1.20	1.17	1.28	1.28	1.24
Total	100.35	99.45	99.42	99.66	99.62	99.59	99.53	99.91	99.96	99.86	99.36	99.19	99	99.24
Sc	8.3	9.1	8.3	6.2	8.3	6.2	5.5	6.1	6.0	5.1	4.4	5.5	5.1	5.2
V	27	36	31	33	24	39	44	42	55	35	38	40	40	27
Cr	10	14	9	10	10	9	9	12	12	19	13	14	13	13
Co	35.4	41.6	41.3	42.3	35.9	70.8	52.4	74.0	53.2	60.0	85.7	56.8	62.9	77.9
Ni	3.2	3.5	4.5	4.4	5.0	9.0	8.1	6.9	10.1	6.5	7.0	4.8	5.2	6.3
Cu	1.0	1.7	1.0	0.6	0.9	2.7	3.3	5.4	7.7	1.4	3.5	3.0	4.0	2.3
Zn	41	53	46	27	35	21	26	25	34	40	33	42	34	33
Ga	16.0	17.9	17.6	14.2	14.9	18.9	19.3	21.1	16.0	17.7	17.5	19.5	19.0	20.7
Rb	77.7	71.3	73.1	81.0	83.0	49.3	57.4	47.2	62.3	51.3	53.1	48.4	50.2	32.4
Sr	465	488	477	586	483	336	477	364	226	214	195.5	218	205	188.5
Y	57.4	58.3	58.6	52.7	53.3	42.3	40.0	39.9	44.1	38.6	41.2	39.7	42.0	42.9
Zr	606	593	609	662	589	488	524	474	498	498	569	480	547	474
Nb	50.5	48.1	48.8	49.0	46.8	40.5	38.6	38.8	40.8	40.3	40.0	40.1	40.3	41.4
Cs	0.94	0.66	0.42	0.44	0.90	2.17	2.25	3.12	2.14	6.18	10.20	8.55	10.80	9.93
Ba	1285	1260	1300	1425	1370	1060	1225	1085	1275	1125	1070	1065	1030	625
La	78.0	79.8	79.7	68.5	71.1	63.1	58.9	59.7	62.9	69.0	65.6	67.5	66.8	68.3
Ce	160	163.5	165.5	149.5	148	130.5	124	123.5	130.5	138.5	134	135	136.5	137
Pr	17.95	18.65	18.85	16.35	16.6	14.85	14.05	14.1	14.7	14.9	14.4	15.1	15	15.1
Nd	69.1	70.3	70.5	60.7	62.6	56	51.6	52.5	54.7	55.8	53.3	55.9	55.8	57
Sm	12.35	13.4	13.25	11.4	11.65	10.3	9.37	9.55	10.3	10.5	9.64	10.3	10.2	10.55
Eu	3.2	3.3	3.3	2.72	3.02	3.22	2.8	2.97	3.22	3.05	2.62	3.38	3.06	3.08
Gd	11.3	11.8	11.75	9.67	10.55	8.61	8.72	8.34	9.17	8.78	8.19	8.96	8.92	8.7
Tb	1.9	1.93	2.02	1.7	1.82	1.45	1.29	1.43	1.56	1.27	1.27	1.32	1.36	1.41
Dy	10.85	11.6	11.45	10.1	10.65	8.53	8.02	7.98	8.82	7.91	8.41	8.21	8.53	9.02
Ho	2.24	2.44	2.43	2.18	2.2	1.79	1.67	1.64	1.8	1.59	1.67	1.67	1.76	1.78
Er	6.45	6.8	6.7	6.11	5.98	4.97	4.66	4.65	5.04	4.81	4.97	4.85	5.02	5.2
Tm	0.97	1	1.01	0.95	0.91	0.76	0.72	0.71	0.82	0.66	0.75	0.69	0.75	0.77
Yb	6.28	6.31	6.52	6.37	5.96	4.84	4.75	4.4	5.29	4.67	5	4.69	5	4.99
Lu	0.98	0.96	1	0.97	0.92	0.81	0.77	0.75	0.81	0.73	0.77	0.71	0.77	0.73
Hf	14.4	14.5	14.8	15.7	14.3	11.9	12.5	11	12.1	11.7	13.6	11.4	13.1	11
Ta	3.62	3.59	3.61	3.89	3.65	3.33	3.25	3.25	3.2	3.46	3.74	3.39	3.55	3.47
Pb	1.1	1.3	1.2	1.2	1	1	1.1	1.1	0.8	2.3	2.7	5.7	2.3	3.6
Th	13.85	13.45	14.2	15.7	13.65	11.65	12.7	11.15	11.8	11.45	13.05	10.7	12.15	10.6
U	3.05	2.97	3.18	3.43	3.06	2.52	2.69	2.44	2.58	2.59	2.94	2.54	2.82	2.59
Σ REE	438.97	450.09	452.58	399.92	405.26	352.03	331.32	332.12	353.73	360.77	351.79	357.98	361.47	366.53
LREE	340.6	348.95	351.1	309.17	312.97	277.97	260.72	262.32	276.32	291.75	279.56	287.18	287.36	291.03
HREE	40.97	42.84	42.88	38.05	38.99	31.76	30.6	29.9	33.31	30.42	31.03	31.1	32.11	32.6
Mg [#]	23.81	22.99	24.36	35.82	26.11	32.62	34.19	32.40	44.45	27.38	28.78	24.28	25.35	26.05

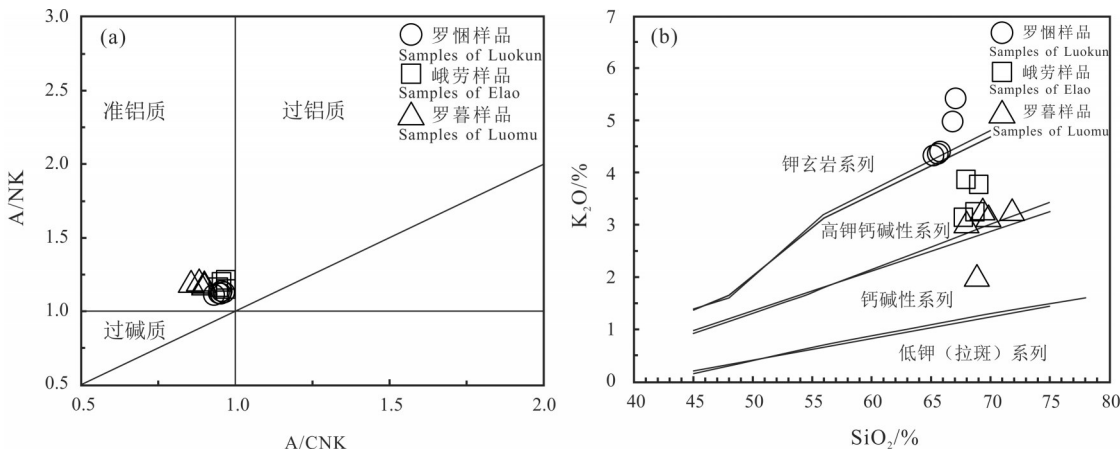


图 5 A/NK-A/CNK 图解(a, 据 Maniar et al., 1989) 及 K₂O-SiO₂ 图解(b, 据 Peccerillo et al., 1976; Middlemost, 1985)
Fig.5 A/NK-A/CNK diagram (a, after Maniar et al., 1989) and K₂O-SiO₂ diagram (b, after Peccerillo et al., 1976; Middlemost, 1985)

点 ²⁰⁷Pb/²⁰⁶Pb 年龄为 2522 Ma、1142 Ma, 其余锆石 ²⁰⁶Pb/²³⁸U 年龄为 965~434 Ma; EL 样品中锆石较古老, ²⁰⁷Pb/²⁰⁶Pb 年龄为 2688~2180 Ma, CL 图像显示锆石具有增生边结构, 推测为继承性来源, 可能反映了早期锆石结晶的记录。而 LM 样品中锆石年龄则较为集中, ²⁰⁶Pb/²³⁸U 年龄为 269~252 Ma。

5.4 Sr-Nd 同位素测试结果

石英二长斑岩的 Sr-Nd 同位素分析结果列于表 4。(⁸⁷Sr/⁸⁶Sr)_i 值和 ε_{Nd(t)} 值根据锆石 U-Pb 年龄 259 Ma 进行计算。样品的 ⁸⁷Sr/⁸⁶Sr 值介于 0.705653~0.707357, (⁸⁷Sr/⁸⁶Sr)_i 值为 0.704247~0.705292, ¹⁴³Nd/¹⁴⁴Nd 值分布于 0.512549~0.512575, ε_{Nd(t)} 值介于 1.08~1.54, Nd 同位素一阶段与二阶段

模式年龄分别为 T_{DM1}=854~905 Ma、T_{DM2}=919~960 Ma。样品 Sr-Nd 同位素位于峨眉山高钛玄武岩和 OIB 范围内, 明显偏离亏损地幔, 并向 EM II 偏移 (图 8), 可能暗示了岩石母岩浆来自于与上地壳组分有关的富集地幔。

6 讨论

6.1 年代学特征

以往报道的研究区及邻区辉绿岩年龄在 263~255 Ma (韩伟等, 2009; 曾广乾等, 2014; 张晓静等, 2014; 祝明金等, 2018), 与 ELIP 喷发时间 (259.1~259.2 Ma, Zhong et al., 2014) 一致。前人对石英二长斑岩进行了锆石同位素年代学研究, 得到岩体年

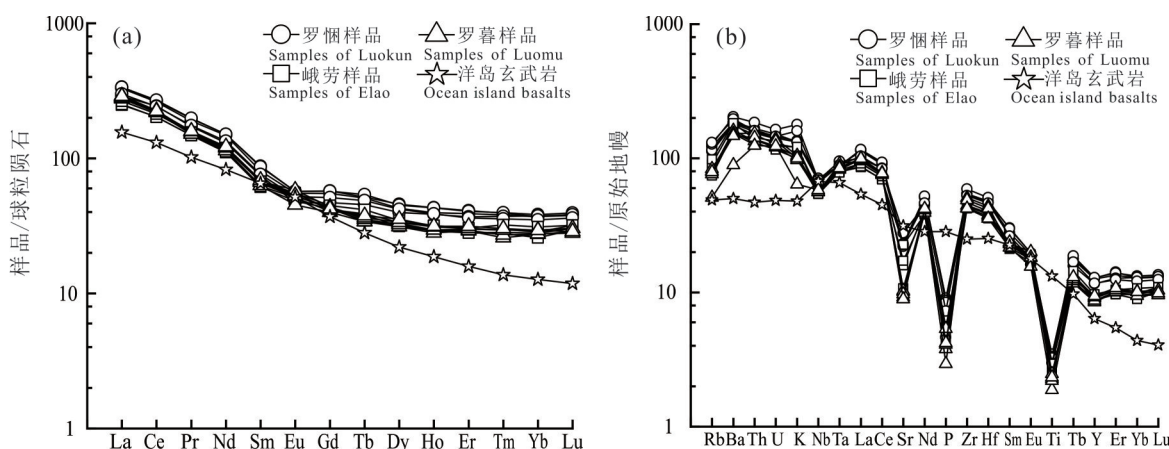


图 6 球粒陨石标准化稀土元素配分图(a)及原始地幔标准化微量元素蛛网图(b)
(OIB 和标准化数值据 Sun et al., 1989)

Fig. 6 Chondrite-normalized REE patterns (a) and primitive mantle normalized spider diagram of trace elements (b)
(OIB and normalizing values after Sun et al., 1989)

表3 锆石SIMS U-Pb测年结果
Table 3 Zircon SIMS U-Pb dating results

测点号	含量/ 10^{-6}			Th/U	同位素比值						年龄/Ma						
	U	Th	Pb		$^{206}\text{Pb} / ^{204}\text{Pb}$	$^{207}\text{Pb} / ^{235}\text{U}$	$\pm\sigma$	$^{206}\text{Pb} / ^{238}\text{U}$	$\pm\sigma$	$^{207}\text{Pb} / ^{206}\text{Pb}$	$\pm\sigma$	$^{207}\text{Pb} / ^{206}\text{Pb}$	$\pm\sigma$	$^{207}\text{Pb} / ^{235}\text{U}$	$\pm\sigma$	$^{206}\text{Pb} / ^{238}\text{U}$	$\pm\sigma$
EL-1	75	92	44	1.227	23201	7.52674	2.66	0.3949	2.35	0.13823	1.25	2205	22	2176	24	2146	43
EL-2	618	224	327	0.363	108116	8.84490	2.64	0.4185	2.13	0.15329	1.55	2383	26	2322	24	2254	41
EL-3	447	237	255	0.531	175727	9.76668	2.19	0.4360	2.09	0.16248	0.66	2482	11	2413	20	2333	41
EL-4	772	426	413	0.552	111019	8.35877	2.16	0.4108	2.13	0.14758	0.39	2318	7	2271	20	2219	40
EL-5	1741	753	1005	0.433	151397	10.28261	3.35	0.4563	3.33	0.16352	0.43	2492	7	2461	32	2423	68
EL-8	359	536	277	1.491	79941	11.57089	2.21	0.4964	2.07	0.16907	0.77	2548	13	2570	21	2598	44
EL-9	644	559	410	0.868	112545	10.46155	4.79	0.4472	4.69	0.16967	1.00	2554	17	2477	45	2383	94
EL-13	160	121	79	0.757	44204	6.96404	3.63	0.3708	3.21	0.13621	1.70	2180	29	2107	33	2033	56
EL-14	64	41	44	0.636	24814	12.45506	4.48	0.5105	3.91	0.17694	2.20	2624	36	2639	43	2659	86
EL-16	787	234	447	0.297	124870	10.44194	1.68	0.4562	1.64	0.16599	0.36	2518	6	2475	16	2423	33
EL-17	438	144	263	0.329	7159	11.92389	2.32	0.4750	2.28	0.18377	0.43	2672	8	2598	22	2505	47
EL-18	455	143	282	0.315	40689	12.41471	2.89	0.4897	2.84	0.18417	0.57	2688	9	2636	28	2569	60
LK-2	3728	77	319	0.021	12349	0.63274	2.85	0.0806	2.78	0.05812	0.54	489	14	498	11	500	13
LK-5	334	497	96	1.490	3380	2.04433	3.50	0.1905	2.48	0.08202	1.83	1142	48	1130	24	1124	26
LK-7	1072	615	214	0.574	52649	1.58804	2.46	0.1615	2.36	0.07133	0.68	967	14	966	15	965	21
LK-9	764	422	66	0.552	31451	0.53742	2.39	0.0705	1.98	0.05531	1.35	425	30	437	9	439	8
LK-10	1767	98	166	0.055	67072	0.69713	2.57	0.0870	2.14	0.05811	1.43	534	31	537	11	538	11
LK-11	2217	68	164	0.031	33958	0.52840	2.41	0.0697	2.26	0.05540	0.78	411	18	431	9	434	10
LK-12	1866	995	161	0.533	8659	0.53877	3.30	0.0711	3.08	0.05663	0.95	410	26	438	12	443	13
LK-13	1239	457	741	0.369	226580	10.78091	3.21	0.4697	3.17	0.16646	0.49	2522	8	2504	30	2482	66
LM-4	4584	9392	318	2.049	6112	0.28995	2.45	0.0412	2.23	0.05339	0.74	240	23	259	6	261	6
LM-11	2165	2786	126	1.287	1089	0.28222	6.54	0.0399	2.55	0.06617	3.17	256	133	252	15	252	6
LM-12	10206	15486	641	1.517	30176	0.29804	2.86	0.0424	2.76	0.05150	0.70	241	17	265	7	268	7
LM-14	3469	5035	216	1.452	3019	0.29331	2.50	0.0413	2.07	0.05642	0.86	266	32	261	6	261	5
LM-15	4959	10028	351	2.022	4233	0.30077	2.50	0.0426	2.14	0.05466	0.84	250	29	267	6	269	6
LM-17	6126	3473	318	0.567	20253	0.29811	3.15	0.0424	3.05	0.05172	0.75	241	19	265	7	268	8

龄分别为(255.2 ± 3.1) Ma(LA-ICP-MS, 黄勇等, 2017)和(164.3 ± 2.4) Ma(LA-MC-ICP-MS, Zhu et al., 2019),在形成年龄方面尚存在较大分歧。在前人的研究结果中,石英二长斑岩样品 $^{206}\text{Pb} / ^{238}\text{U}$ 、 $^{207}\text{Pb} / ^{235}\text{U}$ 和 $^{207}\text{Pb} / ^{206}\text{Pb}$ 三组年龄不一致,且相差较大,反映岩脉可能受到后期热液蚀变的影响或者与测试仪器分辨率和测试精度有关(周红英等,2011)。本文曾挑选新鲜、无明显蚀变的石英二长斑岩样品进行了斜锆石LA-ICP-MS的U-Pb定年(数据未列出),同样出现了3组年龄不一致的情况。综合以上考虑,本文改用分辨率及测年精度更高的SIMS法进行锆石的U-Pb定年。根据野外出露关系来看,石英二长斑岩与围岩辉绿岩界限明显,其年龄与辉绿岩一致或稍晚于辉绿岩年龄。在表3中,可以看到 $^{206}\text{Pb} / ^{238}\text{U}$ 、 $^{207}\text{Pb} / ^{235}\text{U}$ 和 $^{207}\text{Pb} / ^{206}\text{Pb}$ 三组年龄测试结果在误差范围内一致,表明锆石在形成后U-Pb同位素体系封闭性保持较好。在 $^{207}\text{Pb} / ^{235}\text{U}$ 与 $^{206}\text{Pb} / ^{238}\text{U}$ 年龄谐和图上(图9),锆石年龄均分布在谐和曲线上,显示出较好的谐和性,LK

和EL样品中的锆石为继承锆石,年龄数据远大于辉绿岩,LM样品中锆石年龄与辉绿岩年龄接近,计算得到加权平均年龄为(259 ± 2) Ma($n=6$, MSWD=1.08),代表了石英二长斑岩脉的成岩年龄。

6.2 源区性质

石英二长斑岩与辉绿岩在空间上共生,形成年龄一致,表明二者的来源有密切的成因联系。在前人的研究中,辉绿岩($^{87}\text{Sr} / ^{86}\text{Sr}$)值为0.705278~0.706052、 $\varepsilon_{\text{Nd}}(t)$ 值为-0.5~1.6,其母岩浆来自于受地幔柱作用的富集地幔源区,在富集石榴石地幔源区通过部分熔融形成基性岩浆,地壳混染不明显(祝明金等,2018),石英二长斑岩具有较低的($^{87}\text{Sr} / ^{86}\text{Sr}$)值0.704247~0.705292和正的 $\varepsilon_{\text{Nd}}(t)$ 值1.08~1.54与辉绿岩十分相似,显示二者来自同一地幔源区。一般认为,峨眉山高钛玄武岩来自于地幔柱在较大深度(石榴石稳定区)的低度部分熔融,主要分布于地幔柱活动相对较弱的边缘地带(Xu et al., 2001; 徐义刚等,2007)。石英二长斑岩与辉绿岩Sr-Nd同位素组成均位于峨眉山高钛玄武岩的范围内(图8),显

表 4 Sr-Nd 同位素数据
Table 4 Sr-Nd isotopic data

测试项目	样 号									
	LK5-1	LK5-3	LK5-7	LK5-12	LM2-2	LM2-3	LM2-4	LM2-5	LE3-1	LE3-2
Rb /10 ⁻⁶	77.7	71.3	81.0	83.0	53.1	48.4	50.2	32.4	49.3	47.2
Sr /10 ⁻⁶	465.0	488.0	586.0	483.0	195.5	218.0	205.0	188.5	336.0	364.0
⁸⁷ Rb/ ⁸⁶ Sr	0.483432	0.422700	0.399897	0.497164	0.785823	0.642356	0.708488	0.497288	0.424482	0.375106
⁸⁷ Sr/ ⁸⁶ Sr	0.706900	0.706777	0.706759	0.706943	0.707131	0.707357	0.707259	0.707062	0.706529	0.705653
2δ	0.000028	0.000033	0.000036	0.00003	0.000033	0.00003	0.000029	0.000033	0.000035	0.000028
(⁸⁷ Sr/ ⁸⁶ Sr) _i	0.705125	0.705226	0.705292	0.705118	0.704247	0.704999	0.704658	0.705236	0.704971	0.704276
Sm /10 ⁻⁶	12.4	13.4	11.4	11.7	9.6	10.3	10.2	10.6	10.3	9.6
Nd /10 ⁻⁶	69.1	70.3	60.7	62.6	53.3	55.9	55.8	57.0	56.0	52.5
¹⁴⁷ Sm/ ¹⁴⁴ Nd	0.108049	0.115234	0.113540	0.112508	0.109341	0.111392	0.110509	0.111895	0.111194	0.109971
¹⁴³ Nd/ ¹⁴⁴ Nd	0.512559	0.512575	0.512569	0.512551	0.512562	0.512549	0.512555	0.512566	0.512555	0.512571
2δ	0.000015	0.000018	0.000015	0.000017	0.000015	0.000016	0.000016	0.000014	0.000017	0.000017
(¹⁴³ Nd/ ¹⁴⁴ Nd) _i	0.512376	0.512380	0.512377	0.512361	0.512377	0.512361	0.512368	0.512377	0.512367	0.512385
$\varepsilon_{\text{Nd}}(t)$	1.38	1.46	1.39	1.08	1.40	1.08	1.21	1.39	1.20	1.54
T_{DM1}/Ma	855	893	887	905	861	897	882	877	887	854
T_{DM2}/Ma	944	919	928	957	939	960	950	933	950	925

示出峨眉山玄武岩亲缘性,表明石英二长斑岩的原始岩浆来源于地幔柱部分熔融产生的玄武质岩浆。此外,在图8中,样品位于第一象限和第二象限之间,整体向EM II区域偏移,说明岩石的主要混染物质具较高Rb/Sr比值(赵正等,2012),具备这样特

征的岩石可能是上地壳物质(姜寒冰等,2009)。La/Sm和Sm/Yb的比值受分离结晶影响较小,可以有效地指示源区性质(Lassiter et al., 1997),在图10中,样品落在上地壳区域,靠近于尖晶石二辉橄榄岩端元,表明石英二长斑岩原始岩浆在上地壳中与

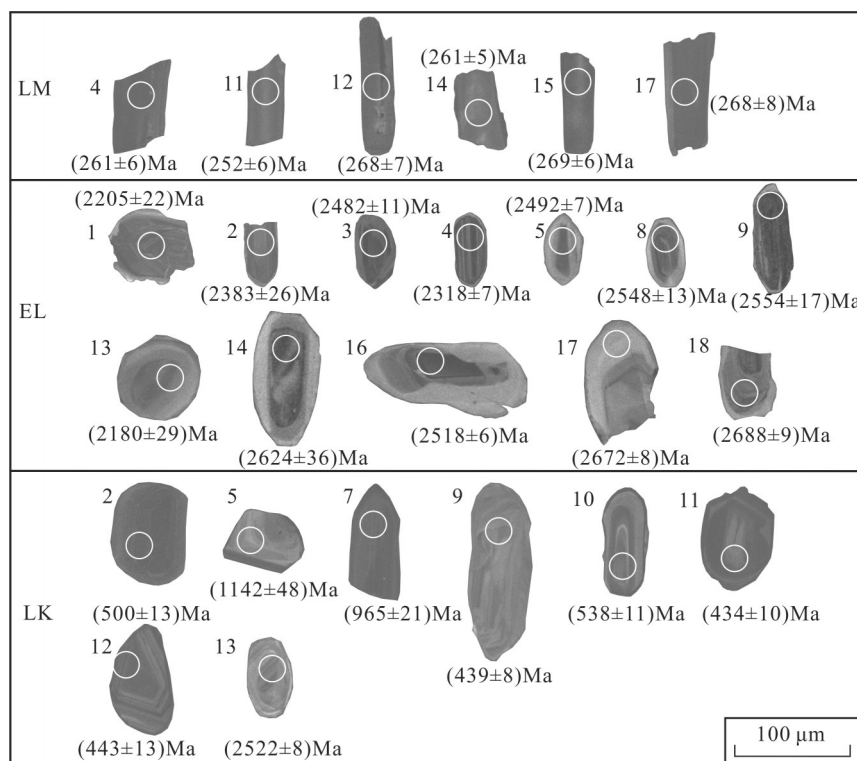
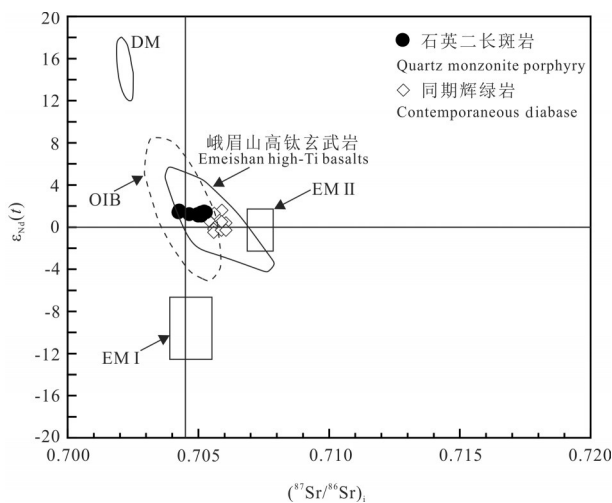


图 7 锆石阴极发光图像
LK—罗甸样品;EL—峨劳样品;LM—罗暮样品
Fig. 7 CL images of zircons
LK—Samples of Luokun; EL—Samples of Elao; LM—Samples of Luomu

图 8 $\varepsilon_{\text{Nd}}(t)$ — $(^{87}\text{Sr}/^{86}\text{Sr})_i$ 图解

(底图据 Condie, 2001; 同期辉绿岩数据来自祝明金等, 2018; DM 数据来自 Zindler et al., 1986; OIB 数据来自 Sun et al., 1989; EM I、EM II 数据来自 Hart et al., 1992; 峨眉山高钛玄武岩数据来自 Xu et al., 2001; Xiao et al., 2004)

Fig. 8 Plot of $\varepsilon_{\text{Nd}}(t)$ — $(^{87}\text{Sr}/^{86}\text{Sr})_i$.

(modified from Condie, 2001; Diabase data from Zhu Mingjin et al., 2018; DM data from Zindler et al., 1986; OIB data from Sun et al., 1989; EM I、EM II data from Hart et al., 1992; The high-Ti Emeishan basalt data from Xu et al., 2001; Xiao et al., 2004)

地壳物质发生了相互作用。石英二长斑岩 Nd 同位素一阶段模式年龄 T_{DM1} 略小于二阶段模式年龄 T_{DM2} (表 4), 岩石形成前后的 Sm/Nd 比值发生了细微的变化 (Liew et al., 1988), 暗示岩浆的演化过程中有地壳物质加入, 同时进一步说明地壳物质加入的量较少。

6.3 岩石成因

岩浆在生成后, 向上运移至侵入地表过程中, 通常会发生分离结晶作用或同化混染作用, 或者同时存在两种作用。样品分异指数 (DI) 为 82.27~88.42, 指示岩石经历了高程度的分异演化作用。石英二长斑岩 $Mg^{\#}$ 为 22.99~44.45 (平均 29.18), 显著低于原始岩浆 (68~75, Frey et al., 1978), 表明岩石形成经历了程度较高的分离结晶作用。在 Harker 图中, 岩石分异演化的趋势明显, 部分元素的趋势线的斜率随分异程度的改变发生变化 (图 11), 指示岩浆演化不同阶段分离的矿物组合有所差异。 MgO 、 TFe_2O_3 、 TiO_2 、 P_2O_5 与 SiO_2 呈负相关, 表明在岩浆演化过程中, 存在镁铁矿物、钛铁氧化物及磷灰石等分离结晶, 而 CaO 与 SiO_2 的正相关则可能暗示存在地壳物质同化混染作用的影响。样品 Eu、Nb、Ta、Sr、P、Ti 等元素的相对亏损 (图 6), 表明存在斜长石、金红石或钛铁矿等矿物的分离结晶。Nb/U 值是判别火成岩是否受到地壳混染的有效指示参数 (Hofmann et al., 1986; Campbell, 2002), Nb/U 数值越低遭受地壳混染程度越大, 如大洋玄武岩和原始地幔 Nb/U 值分别为 47 和 34 (Sun et al., 1989), 而整体地壳 Nb/U 约为 6 (Rudnick et al., 2003)。石英二长斑岩的 Nb/U 比值为 13.61~16.56 (平均 15.36), 说明石英二长斑岩形成过程中受到地壳物质的混染。Zr 的丰度随分异作用而增加, Th/Nb 比值几乎不受影响, 根据 Zr 与 Th/Nb 比值的协变关系, 可以准确地检验是否存在同化混染作用, 并判断同化混

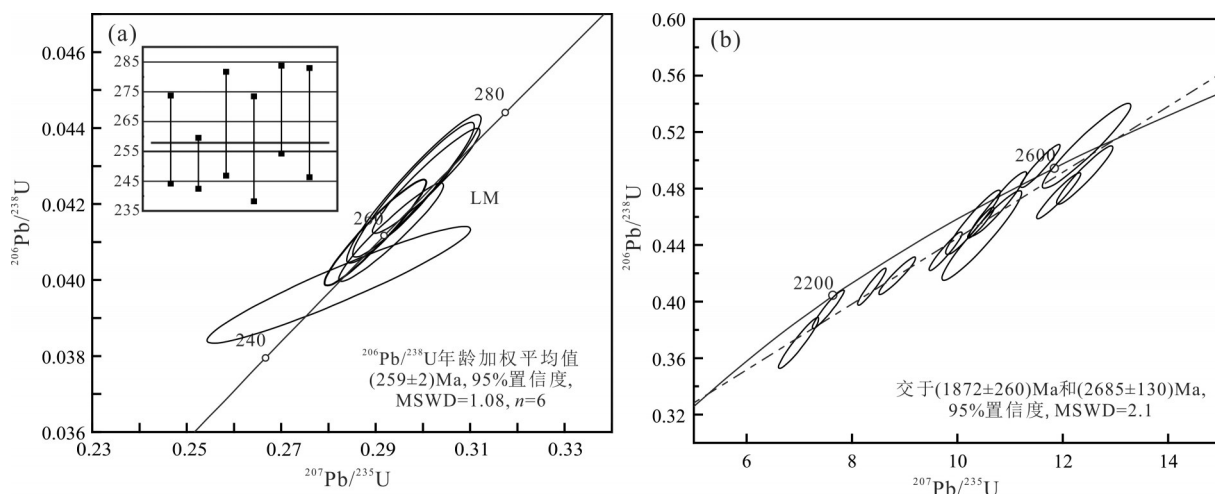


图 9 锆石 SIMS U-Pb 年龄谐和图
Fig.9 Concordia curves of Zircons SIMS U-Pb data

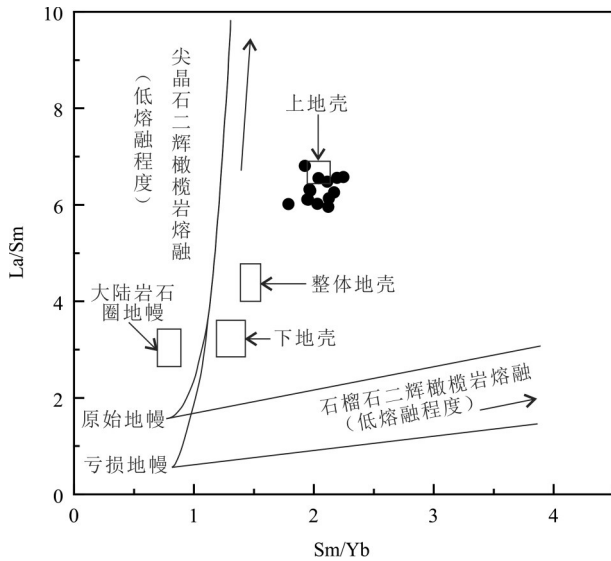


图 10 La/Sm-Sm/Yb 图解

(底图据 Lassiter et al., 1997; 原始地幔和亏损地幔据 Mckenzie et al., 1991; 大陆岩石圈地幔据 McDonough, 1990; 上、下地壳和整体地壳据 Taylor et al., 1995)

Fig.10 Diagram of La/Sm-Sm/Yb
(modified from Lassiter et al., 1997; Primary mantle and depleted mantle are after Mckenzie et al., 1991; Continental lithospheric mantle are after McDonough, 1990; Upper crust, Lower crust and Bulk crust are after Taylor et al., 1995)

染程度 (Barker et al., 1997; Mcdonald et al., 2001)。样品中较高的 Zr 含量 $474 \times 10^{-6} \sim 662 \times 10^{-6}$ 与较低的 Th/Nb 比值 0.26~0.27, 在 Zr-Th/Nb 图解(图 12)中所有投点的趋势线随分异程度的增加略有上

升, 显示岩石成因主要受分离结晶影响, 并伴有较低程度的同化混染。此外, 样品中古老继承锆石的存在, 也指示在成岩过程中受到了壳源物质的混染 (Samson et al., 2018; Olierook et al., 2020)。

ELIP 岩浆活动零星出露中酸性火山岩, 与基性火山岩共生 (邵辉等, 2007; Xu et al., 2010), 有学者认为酸性端元和基性端元来自于不同母岩浆, 是地幔柱来源的基性岩浆大量底侵导致下地壳物质部分熔融的产物, 这种情况下中酸性端元出露面积较大 (邵辉等, 2007; Shellnutt et al., 2010; 骆文娟等, 2011; 徐义刚等, 2013)。虽然微量元素、Sr-Nd 同位素及大量继承锆石的证据都表明石英二长斑岩的形成存在地壳物质贡献, 但是本文的证据并不支持这一熔融成因模式, 因为罗甸石英二长斑岩比同期辉绿岩出露规模小得多, 同位素和微量元素的分析也表明混染物质来自上地壳。也有研究者认为二者有相同母岩浆, 酸性端元由基性岩浆分离结晶作用形成, 并可伴有一定量的地壳物质加入, 生成的酸性端元岩浆规模要小得多 (Frost et al., 2001; Bonin et al., 2007; 钟宏等, 2009; Zhong et al., 2011), 这一模式更符合罗甸石英二长斑岩的证据事实。综合前文所述, 石英二长斑岩的原始岩浆来自于受地幔柱作用的地幔源区, 地幔热柱在较大深度经低程度部分熔融形成玄武质岩浆, 并经历了较高程度的分离结晶演化过程, 在到达地表的过程中

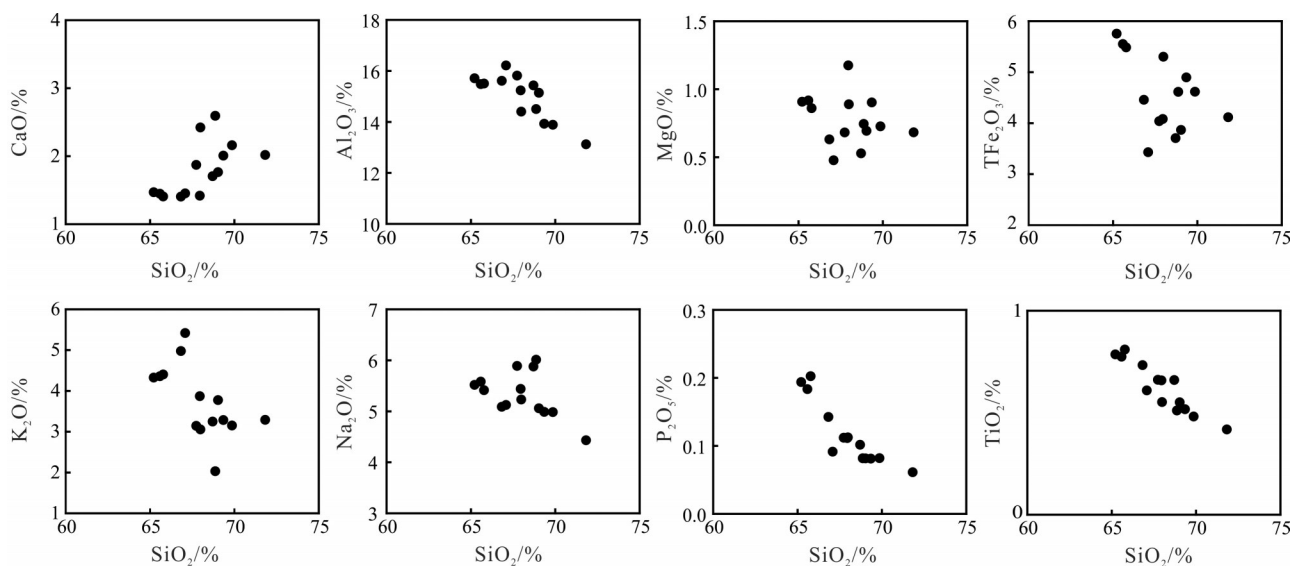


图 11 Harker 图解

Fig.11 Harker diagram

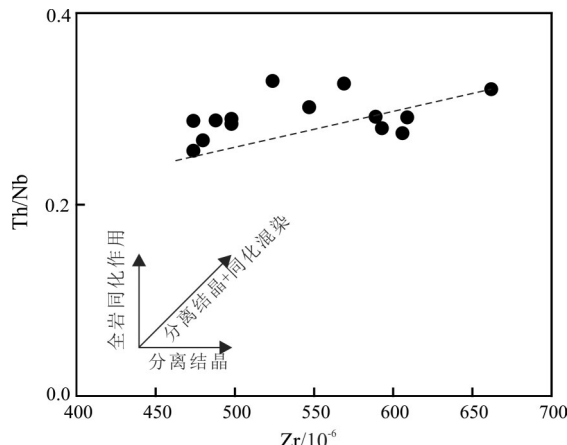


图 12 Th/Nb-Zr 图解
Fig.12 Plot of Th/Nb-Zr

混染了少量上地壳物质后,最终以岩脉的形式侵位于同期辉绿岩中。其动力机制可能与区域构造活动创造了侵位通道有关,因为研究区出露相当规模的辉绿岩岩墙群反映了当时伸展拉张的环境(韩伟等,2009),为酸性岩浆的侵位提供了有利条件。

6.4 与 ELIP 岩浆活动的关系

峨眉山大火成岩省位于扬子地块西南部,广泛分布于四川、云南、贵州三省,前人对其岩石系列、岩浆起源及源区特征、地幔柱动力学、二叠纪生物大灭绝事件和岩浆成矿作用的关系开展了大量研究工作(王登红等,2001,2004; Ali et al., 2002; 张招崇等, 2005; 李宏博等, 2010; He et al., 2010; Shellnutt et al., 2010; 徐义刚等, 2013; 朱江等, 2013)。从以往的研究来看,中酸性岩体主要分布于ELIP分布区域内带,如攀西地区营盘梁子花岗岩、二郎河花岗岩、白马正长岩体、攀枝花正长岩体和花岗岩体、太和花岗岩体、茨达复式岩体的中酸性岩体、米易正长岩体、会理猫猫沟霞石正长岩体、云南富民中性岩(罗震宇等, 2006; Shellnutt et al., 2007, 2011; Xu et al., 2008; Zhou et al., 2008; Zhong et al., 2009; 骆文娟等, 2011; 李宏博等, 2015)等。峨眉山大火成岩省精确的主喷发期限定在259.1~259.2 Ma (Zhong et al., 2014),持续时间小于1 Ma。罗甸石英二长斑岩形成年龄(259±2)Ma,与峨眉山大火成岩省岩浆活动时间一致。一般认为中酸性岩体出现在ELIP活动的晚期(邵辉等, 2007; 徐义刚等, 2013; 李宏博等, 2015),与地幔柱活动晚期岩浆供给少,在地壳岩浆房中停留时间长,岩浆发生强

烈分离结晶作用有关(Li Jie et al., 2010),这与罗甸石英二长斑岩显示出的分离结晶和地壳混染的特征吻合。前人认为ELIP中酸性岩浆作用可能具有普遍性,地幔柱岩浆作用是复杂且多样的(李宏博等,2015),对位于ELIP外带的罗甸石英二长斑岩进行的研究为这一观点提供了新证据。

6.5 古老锆石的讨论

石英二长斑岩中存在大量古老的继承性锆石,虽然其年龄数据比较分散,但仍然是以往的地质历史中构造事件记录的载体。在年龄谐和图上,古老锆石均显示出较好的谐和性(图9b)。样品的古老锆石年龄分布有一定规律,可大致分为3组(图7):(1)(2688±9) Ma ~ (2180±29) Ma; (2)(1142±48) Ma ~ (965±21) Ma; (3)(500±13) Ma ~ (434±10) Ma。查阅资料发现,古老锆石的出现可能是对扬子地块不同阶段构造活动的响应:

第(1)组年龄对应新太古代—古元古代。在扬子地块内,古元古代岩石主要分布在扬子地块北缘和西南缘,与Columbia超大陆聚合-裂解密切相关(邓奇等,2020),如扬子地块北缘崆岭2.15~2.14 Ga的蛇绿混杂岩(Han et al., 2019)、2.00~1.93 Ga花岗岩(Wang et al., 2019)和扬子西南缘大红山2.0 Ga弧岩浆岩(Kou et al., 2017)等。

第(2)组年龄对应新元古代。华南板块包含了扬子地块、江南造山带和华夏地块,其中的江南造山带是华夏洋壳(华南洋)俯冲到扬子地块之下所引起的增生和碰撞造山作用的产物(Zhang et al., 2013)。华南洋开始消减的时限大约为1200 Ma,碰撞的高峰期在1000~950 Ma(吴根耀, 2000)。在中元古代末到新元古代初的武陵运动(1050~1000 Ma)中,华南洋向扬子陆块俯冲,在扬子地块东南部形成增生的构造带,在华夏地块西北边缘形成了陆缘弧盆系(韩伟, 2010; 杨明桂等, 2015)。在约970 Ma时,扬子至华夏地块之间的华南洋在扬子地块的东部消失,形成江山—绍兴段缝合带(李献华等, 1996, 1999),而在扬子地块西南部则仍残留下一个盆地,除钦防槽盆外的整个盆地至中奥陶世逐渐关闭,至志留纪末形成了统一的华南加里东构造带(汪正江, 2008)。

第(3)组年龄对应奥陶纪—志留纪。在贵州境内的都匀运动发生于奥陶纪末到志留纪初,表现为

挤压背景下的大面积抬升运动,使得黔中隆起和黔南坳陷抬升成陆;发生于志留纪末的广西运动则使黔中、黔南整体继续隆升,隆起范围进一步扩大(崔金栋,2013)。

此外,值得注意的是,本次研究中最古老的一颗锆石年龄为(2688 ± 9)Ma,这是目前在扬子地块西南缘贵州境内南部火成岩中发现的最古老的继承锆石,可以为扬子地块存在太古代基底提供锆石年代学方面的依据。

7 结 论

(1)石英二长斑岩锆石SIMS测年结果为(259 ± 2)Ma,与区内辉绿岩年龄和ELIP喷发时间一致。Sr-Nd同位素及微量元素特征表明,岩石与辉绿岩的具有相同的母岩浆,来自同一地幔源区。石英二长斑岩是由地幔柱部分熔融产生的玄武质岩浆经历分离结晶的产物,并混染了少量上地壳物质。

(2)罗甸石英二长斑岩的发现,说明ELIP中酸性岩浆作用可能具有普遍性。古老锆石的出现可能为扬子地块不同阶段构造活动的响应,同时也为扬子地块存在太古宙古老基底提供锆石年代学方面的依据。

致谢:论文撰写和修改过程中得到了冯光英副研究员、吴伟伟博士的悉心指导和帮助;审稿专家对本文提出了许多宝贵的意见,在此一并致以衷心的感谢!

注释

① 广西区域地质测量队区域地质测量队. 1972. 1:20万乐业幅地质图[R]. 广西壮族自治区地质局.

Reference

- Ali J R, Thompson G M, Song Xieyan, Wang Yuliang. 2002. Emeishan basalts (SW China) and the ‘end-Guadalupian’ crisis: Magnetobiostratigraphic constraints[J]. Journal of the Geological Society, 159: 21–29.
- Ali J R, Thompson G M, Zhou Meifu, Song Xieyan. 2005. Emeishan large igneous province, SW China[J]. Lithos, 79:475–489.
- Barker J A, Menzies M A, Thirlwall M F, Macpherson C G. 1997. Petrogenesis of Quaternary intraplate volcanism, Sana'a Yemen: Implication and polybaric melt hybridization[J]. Journal of Petrology, 38: 1359–1390.
- Bonin B. 2007. A-type granites and related rocks: Evolution of a concept, problems and prospects[J]. Lithos, 97: 1–29.
- Bryan S E, Ernst R E. 2008. Revised definition of Large Igneous Provinces (LIPs)[J]. Earth-Science Review, 86(1/4): 175–202.
- Bryan S E, Ewart A, Stephens C J, Parianos J, Downes P J. 2000. The Whitsunday volcanic province, Central Queensland, Australia: Lithological and stratigraphic investigations of a silicic-dominated large igneous province[J]. Journal of Volcanology and Geothermal Research, 99(1/4): 55–78.
- Bryan S E, Peate I U, Peate D W, Self S, Jerram D A, Mawby M R, Marsh J S, Miller J A. 2010. The largest volcanic eruptions on Earth[J]. Earth-Science Reviews, 102(3/4): 207–229.
- Bureau of Geology and Mineral Exploration and Development Guizhou Province. 1987. Regional Geology of Guizhou Province[M]. Beijing: Geological Publishing House, 554–596 (in Chinese).
- Campbell I H. 2002. Implications of Nb/U, Th/U and Sm/Nd in plume magmas for the relationship between continental and oceanic crust formation and the development of the depleted mantle[J]. Geochimica et Cosmochimica Acta, 66, 1651–1661.
- Chung Sunlin, Jahn B M, Wu Genyao, Lo C H, Cong B L. 1998. The Emeishan flood basalt in SW China: A mantle plume initiation model and its connection with continental breakup and mass extinction at the Permian-Triassic boundary[C]//Mantle Dynamics and Plate Interactions in East Asia. American Geophysical Union Geodynamics Series, 27, 47–58.
- Condie K C. 2001. Mantle Plumes and Their Record in Earth History[M]. Cambridge University Press.
- Cui Jindong. 2013. Sedimentary Response to Tectonic Evolution of the Central Guizhou Uplift and Its Adjacent Areas[D]. Changsha: Central South University (in Chinese with English abstract).
- Deng Qi, Wang Zhengjiang, Ren Guangming, Cui Xiaozhuang, Cao Huawen, Ning Kuobu, Ren Fei. 2020. Identification of the ~2.09 Ga and ~1.76 Ga granitoids in the Northwestern Yangtze Block: Records of the assembly and break-up of Columbia supercontinent[J]. Earth Science, 45(9): 3295–3312 (in Chinese with English abstract).
- Ernst R E, Buchan K L, Campbell I H. 2005. Frontiers in large igneous province research[J]. Lithos, 79(3/4): 271–297.
- Frey F A, Green D H, Roy S D. 1978. Integrated models of basalt petrogenesis: A study of quartz tholeiites to olivine melilitites from south eastern Australia utilizing geochemical and experimental petrological data[J]. Journal of Petrology, 19 (3): 463–513.
- Frost C D, Bell J M, Frost B R, Chamberlain K R. 2001. Crustal growth by magmatic underplating: Isotopic evidence from the northern Sherman batholith[J]. Geology, 29: 515–518.
- Han Qingsen, Peng Songbai, Polat A, Kusky T. 2019. Petrogenesis and geochronology of paleoproterozoic magmatic rocks in the Kongling Complex: Evidence for a collisional orogenic event in the Yangtze Craton[J]. Lithos, 342–343: 513–529.
- Han Wei. 2010. Tectonic Evolution and Geological Significance of

- Ziyun– Luodian– Nandan Rift Zone[D]. Xi'an: Northwest University (in Chinese with English abstract).
- Han Wei, Luo Jinhai, Fan Junlei, Cao Yuanzhi, Zhang Jingyi. 2009. Late Permian diabase in Luodian, Southeastern Guizhou, and its tectonic significances[J]. *Geological Review*, 55(6): 795–803 (in Chinese with English abstract).
- Hao Jiaxu, Zhang Guoxiang, Han Yingping, Deng Xiaojie, Jiang Yanxia, Qiang Xirun. 2014. Discovery of intermediate magma and its significance in South Guizhou[J]. *Guizhou Geology*, 36(1): 52–55 (in Chinese with English abstract).
- Hart S R, Hauri E H, Oschmann L A, Whitehead J A. 1992. Mantle plumes and entrainment: Isotopic evidence[J]. *Science*, 256: 517–520.
- He Bin, Xu Yigang, Chung Sunling, Xiao Long, Wang Yamei. 2003. Sedimentary evidence for a rapid, kilometer-scale crustal doming prior to the eruption of the Emeishan flood basalts[J]. *Earth and Planetary Science Letters*, 213(3/4): 391–405.
- He Bin, Xu Yigang, Zhong Yuting, Guan Junpeng. 2010. The Guadalupian– Lopingian boundary mudstones at Chaotian (SW China) are clastic rocks rather than acidic tuffs: Implication for a temporal coincidence between the end- Guadalupian mass extinction and the Emeishan volcanism[J]. *Lithos*, 119(1/2):10–19.
- Heaman L M, Lecheminant A N. 1993. Paragenesis and U– Pb systematics of baddeleyite (ZrO_2) [J]. *Chemical Geology*, 110(1/3): 95–26.
- Huang Yong, Chen Nengsong, Dai Chuangu, Han Yingping, Bai Long, Deng Xiaojie. 2017. Zircon U– Pb dating and its significance of intermediate intrusive rocks within the basic sill in Luodian Nephrite Deposit, Guizhou Province[J]. *Guizhou Geology*, 34(2): 90–96 (in Chinese with English abstract).
- Hofmann A W, Jochum K P, Seufert M, White W M. 1986. Nb and Pb in oceanic basalts: New constraints on mantle evolution[J]. *Earth and Planetary Science Letters*, 79: 33–45.
- Jiang Hanbing, Jiang Changyi, Qian Zhuangzhi, Zhu Shifei, Zhang Pengbo, Tang Dongmei. 2009. Petrogenesis of high–Ti and low–Ti basalts in Emeishan, Yunnan, China[J]. *Acta Petrologica Sinica*, 25 (5): 1117–1134 (in Chinese with English abstract).
- Kou Caihua, Zhang Zhaochong, Santosh M, Huang He, Zhu Jiang. 2017. Oldest volcanic–hosted submarine iron ores in South China: Evidence from zircon U– Pb geochronology and geochemistry of the Paleoproterozoic Dahongshan Iron Deposit[J]. *Gondwana Research*, 49: 182–204.
- Lassiter J C, Depaolo D J. 1997. Plume/lithosphere interaction in the generation of continental and oceanic flood basalts: Chemical and isotope constraints[C]//Mahoney J(eds.). *Large Igneous Provinces: Continental, Oceanic and Planetary Flood Volcanism*. USA: American Geophysical Union: Geophysical Monograph, 100, 335–55.
- Li Hongbo, Zhang Zhaochong, Li Yongsheng. 2015. Geochronology and geochemistry of the Late Permian intermediary– mafic intrusions in Fumin, Yunnan Province: Implications for the magmatism of Emeishan large igneous province[J]. *Acta Geologica Sinica*, 89(1): 18–36 (in Chinese with English abstract).
- Li Jie, Xu Jifeng, Suzuki K, He Bin, Xu Yigang, Ren Zhongyuan. 2010. Os, Nd and Sr isotope and trace element geochemistry of the Muli picrites: Insights into the mantle source of the Emeishan large igneous province[J]. *Lithos*, 119(1/2): 108–122.
- Li Xianhua. 1996. Nd isotopic evolution of sediments from the southern margin of the Yangtze block and its tectonic significance[J]. *Acta Petrologica Sinica*, 12(3): 359–369 (in Chinese with English abstract).
- Li Xianhua, Lee Chiyu, Liu Ying, Chen Duofu, Wang Yixian, Zhao Zhenhua. 1999. Geochemistry characteristics of the Paleoproterozoic meta–volcanics in the Cathaysia block and its tectonic significance[J]. *Acta Petrologica Sinica*, 15(3): 364–371 (in Chinese with English abstract).
- Li Xianhua, Liu Yu, Li Qiu, Guo Chunhua, Kevin R C. 2009. Precise determination of Phanerozoic zircon Pb/Pb age by multicollector SIMS without external standardization [J]. *Geochemistry Geophysics Geosystems*, 10(4): Q04010.
- Liew T C, Hofmann A W. 1988. Precambrian crustal components, plutonic associations, plate environment of the Hercynian fold belt of central Europe: Indications from a Nd and Sr isotopic study[J]. *Contributions to Mineralogy & Petrology*, 98(2): 129–138.
- Ludwig K R. 2003. Isoplot/Ex version 2.49: A geochronological toolkit for Microsoft Excel[M]. Berkeley Geochronology Center Special Publication, 1: 1–56.
- Luo Wenjuan, Zhang Zhaochong, Hou Tong, Wang Meng. 2011. Geochronology and geochemistry of the Cida complex in the Panxi district: Constraints on the duration of the Emeishan mantle plume[J]. *Acta Petrologica Sinica*, 27(10): 2947–2962 (in Chinese with English abstract).
- Luo Zhenyu, Xu Yigang, He Bin, Shi Yuruo, Huang Xiao. 2006. On the genetic relationship between Maomaogou nepheline syenite in Panxi and Emeishan igneous province: Evidence from geochronology and rock geochemistry[J]. *Chinese Science Bulletin*, 51(15): 1802–1810 (in Chinese).
- Middlemost E A K. 1985. *Magmas and Magmatic Rocks: An Introduction to Igneous Petrology*[M]. London: Longman, 1–266.
- Middlemost E A K. 1994. Naming materials in the magma/igneous rock system[J]. *Earth–Science Review*, 37(3/4): 215–224.
- Maniar P D, Piccoli P M. 1989. Tectonic discrimination of granitoids[J]. *Geological Society of America Bulletin*, 101(5): 635–643.
- Li Hongbo, Zhang Zhaochong, Lü Linsu. 2010. Geometry of the mafic dyke swarms in Emeishan large igneous province: Implications for mantle plume[J]. *Acta Petrologica Sinica*, 26(10): 3143–3152 (in Chinese with English abstract).

- McDonough W F. 1990. Constraints on the composition of the continental lithospheric mantle[J]. *Earth and Planetary Science Letters*, 101: 1–18.
- McKenzie D P, O'Nions R K. 1991. Partial melt distribution of melt generated by rare earth element concentrations[J]. *Journal of Petrology*, 21: 1021–1091.
- Macdonald R, Rogers N W, Fitton J G, Black S, Smith M. 2001. Plume–lithosphere interactions in the generation of the basalts of the Kenya Rift, East Africa[J]. *Journal of Petrology*, 2001 (5): 877–900.
- Olieroor H K H, Kirkland C L, Szilas K, Hollis J A, McDonald B J. 2020. Differentiating between inherited and autocrytic zircon in granitoids[J]. *Journal of Petrology*, 61(8): egaa081.
- Peccerillo A, Taylor S R. 1976. Geochemistry of Eocene calc-alkaline volcanic rocks from the Kastamonu area, Northern Turkey[J]. *Contributions to Mineralogy and Petrology*, 58(1): 63–81.
- Rudnick R L, Gao S. 2003. The composition of the continental crust[C]//Rudnick R L(ed.). *The Crust*. Oxford: Elsevier Pergamon, 1–64.
- Samson S D, Moehler D P, Satkoski A M. 2018. Inherited, enriched, heated, or recycled? Examining potential causes of Earth's most zircon fertile magmatic episode[J]. *Lithos*, 314: 350–359.
- Shao hui, Xu Yigang, He Bin, Huang Xiaolong, Luo Zhenyu. 2007. Petrology and geochemistry of the late-stage acidic volcanic rocks of the Emeishan large igneous province[J]. *Bulletin of Mineralogy, Petrology and Geochemistry*, 26(4): 350–358 (in Chinese with English abstract).
- Shellnutt J G, Jahn B M. 2010. Formation of the Late Permian Panzhihua plutonic–hypabyssal–volcanic igneous complex: Implications for the genesis of Fe–Ti oxide deposits and A-type granites of SW China[J]. *Earth and Planetary Science Letters*, 289 (3/4): 509–519.
- Shellnutt J G, Jahn B M, Zhou Meifu. 2011. Crustal-derived granites in the Panzhihua region, SW China: Implications for felsic magmatism in the Emeishan large igneous province[J]. *Lithos*, 123: 145–157.
- Shellnutt J G, Zhou Meifu. 2007. Permian peralkaline, peraluminous and metaluminous A-type granites in the Panxi district, SW China: Their relationship to the Emeishan mantle plume[J]. *Chemical Geology*, 243: 286–316.
- Sláma J, Košler J, Condon D J, Crowley J L, Gerdes A, Hanchar J M, Horstwood M S A, Morris G, Naadala L, Norberg N, Schaltegger U, Schoene B, Tubrett M, Whitehouse M J. 2008. Pleovice zircon: A new natural reference material for U–Pb and Hf isotopic microanalysis[J]. *Chemical Geology*, 249(1): 1–35.
- Song Xieyan, Qi Huawen, Robinson P T, Zhou Meifu, Cao Zhimin, Chen Leimeng. 2008. Melting of the subcontinental lithospheric mantle by the Emeishan mantle plume: Evidence from the basal alkaline basalts in Dongchuan, Yunnan, Southwestern China[J]. *Lithos*, 100: 93–111.
- Stacey J S, Kramers J D. 1975. Approximation of terrestrial lead isotope evolution by a 2–stage model[J]. *Earth and Planetary Science Letters*, 26(2): 207–221.
- Sun S S, McDonough W F. 1989. Chemical and isotopic systematics of oceanic basalts: Implications for mantle composition and processes[J]. *Geological Society of London Special Publication*, 42 (1): 313–345.
- Taylor S R, McLennan S M. 1995. The geochemical evolution of the continental crust[J]. *Reviews of Geophysics*, 33(2): 241–265.
- Wang Denghong. 2001. Basic concept, classification, evolution of mantle plume and large scale mineralization—probe into southwestern China[J]. *Earth Science Frontiers*, 8(3): 67–72 (in Chinese with English abstract).
- Wang Denghong, Li Jiankang, Liu Feng, Chen Zhenyu. 2004. Some problems related to mantle plume and their significance in ore prospecting[J]. *Acta Geoscientica Sinica*, 25(5): 489–494 (in Chinese with English abstract).
- Wang Kai, Dong Shuwen. 2019. New insights into Paleoproterozoic tectonics of the Yangtze Block in the context of Early Nuna assembly: Possible collisional granitic magmatism in the Zhongxiang complex, South China[J]. *Precambrian Research*, 334: 105452.
- Wang Shangyan, Zhang Hui, Peng Chenglong, Chen Minghua, Shi Lei, Zhang Quanli, Wang Hongmei, Wang Tianhua, Wang Chunhou, Hu Renfa. 2005. Evolution of Palaeo-Mesozoic Strata and Rifting Basins in Western Guizhou[M]. Beijing: Geological Publishing House (in Chinese).
- Wang Shangyan, Zhang Hui, Wang Tianhua, Wang Chunhou, Peng Chenglong, Hu Renfa, Chen Minghua, Shi Lei. 2006. Filling and evolution of the Late Paleozoic Shuicheng–Ziyun aulacogen in western Guizhou, China[J]. *Geological Bulletin of China*, 25(3): 402–407 (in Chinese with English abstract).
- Wang Zhengjiang. 2008. Neoproterozoic Rift Basin Evolution and its Stratigraphic Division and Correlation in Eastern Guizhou[D]. Beijing: Chinese Academy of Geological Sciences (in Chinese with English abstract).
- Wingate M Y D, Compston W. 2000. Crystal orientation effects during ion microprobe U–Pb analysis of Baddeleyite[J]. *Chemical Geology*, 168(1/2): 75–97.
- Wu Genyao. 2000. Grenville orogens in south China and their collapse: Implications for evolution of the Supercontinent Rodinia[J]. *Geotectonica et Metallogenesis*, 24(2): 112–123 (in Chinese with English abstract).
- Xiao Long, Xu Yigang, Chung Sunlin, He Bin, Mei Houjun. 2003. Chemostratigraphic correlation of Upper Permian lava succession from Yunnan Province, China: Extent of the Emeishan large igneous province[J]. *International Geology Review*, 45: 753–766.
- Xiao Long, Xu Yigang, Mei H J, Zheng Yongfei, He Bin, Pirajno F. 2004. Distinct mantle sources of low-Ti and high-Ti basalts from the western Emeishan large igneous province, SW China: Implications for plume–lithosphere interaction[J]. *Earth & Planetary Science Letters*, 228(3/4): 525–546.

- Xu Yigang, Chung Sunlin, Jahn Borning, Wu Genyao. 2001. Petrologic and geochemical constraints on the petrogenesis of Permian–Triassic Emeishan flood basalts in southwestern China[J]. *Lithos*, 58(3/4): 145–168.
- Xu Yigang, Chung Sunlin, Shao Hui, He Bin. 2010. Silicic magmas from the Emeishan large igneous province, Southwest China: Petrogenesis and their link with the end-Guadalupian biological crisis[J]. *Lithos*, 119(1/2): 47–60.
- Xu Yigang, He Bin, Huang Xiaolong, Luo Zhenyu, Zhu Dan, Ma Jinlong, Shao Hui. 2007. The debate over mantle plumes and how to test the plume hypothesis[J]. *Earth Science Frontiers*, 14(2): 1–9 (in Chinese with English abstract).
- Xu Yigang, He Bin, Luo Zhenyu, Liu Haiquan. 2013. Study on mantle plume and large igneous provinces in China: An overview and perspectives[J]. *Bulletin of Mineralogy, Petrology and Geochemistry*, 32(1): 25–39 (in Chinese with English abstract).
- Xu Yigang, Luo Zhenyu, Huang Xiaolong, He Bin. 2008. Zircon U–Pb and Hf isotope constraints on crustal melting associated with Emeishan mantle plume[J]. *Geochimica et Cosmochimica Acta*, 72(13): 3084–3104.
- Yang Minggui, Yu Zhongzhen, Xu Meigui, Tang Weixin, Wang Guanghui, Hu Qinghua. 2015. Tectonic framework of Huanan Ocean in the Jinning period[C]// The 13th Geoscience and Technology Forum of Six Provinces and One City in East China, Jiangxi: Geological Society of Jiangxi Province, 1–17 (in Chinese with English abstract).
- Zeng Guangqian, He Lianglun, Yang Kunguang. 2014. Geochronology, geochemistry and geological significances of diabase dykes in Pu’An, West Guizhou[J]. *Journal of Mineralogy and Petrology*, 34(4): 61–70 (in Chinese with English abstract).
- Zhang Qingwen, Zhu Dan, Xu Yingkui. 2015. Heat source for continental crust melting and silicic magma generation[J]. *Acta Mineralogica Sinica*, 35(1): 44–50 (in Chinese).
- Zhang Shaobing, Zheng Yongfei. 2013. Formation and evolution of Precambrian continental lithosphere in South China[J]. *Gondwana Research*, 23: 1241–1260.
- Zhang Xiaojing, Xiao Jiafei. 2014. Zircon U–Pb Geochronology, Hf isotope and geochemistry study of the Late Permian diabases in the Northwest Guangxi Autonomous Region[J]. *Bulletin of Mineralogy, Petrology and Geochemistry*, 33(2): 163–176 (in Chinese with English abstract).
- Zhang Zhaochong, Mao Jingwen, Cai Jinhong, Kusky T M, Zhou Gang, Yan Shenghao, Zhao Li. 2006. Geochemistry of picritic and associated basalt flows of the western Emeishan flood basalts province, China[J]. *Journal of Petrology*, 47(10): 1997–2019.
- Zhang Zhaochong, Wang Fusheng, Fan Weiming, Deng Hailin, Xu Yigang, Xu Jifeng, Wang Yuejun. 2001. A discussion on some problems concerning the study of the Emeishan basalts[J]. *Acta Petrologica et Mineralogica*, 20(3): 239–246 (in Chinese with English abstract).
- Zhang Zhaochong, Wang Fusheng, Hao Yanli. 2005. Picrites from the Emeishan large igneous province: Evidence for the mantle plume activity[J]. *Bulletin of Mineralogy, Petrology and Geochemistry*, 24(1): 17–22 (in Chinese with English abstract).
- Zhao Zheng, Qi Liang, Huang Zhilong, Yan Zaifei, Xu Cheng. 2012. Trace elements and Sr–Nd isotopic geochemistry and genesis of Jijie alkaline-ultramafic rocks, southern part of Panxi rift[J]. *Acta Petrologica Sinica*, 28(6): 1915–1927 (in Chinese with English abstract).
- Zhong Hong, Campbell I H, Zhu Weiguang, Charlotte M A, Hu Ruizhong, Xie Liewen, He Defeng. 2011. Timing and source constraints on the relationship between mafic and felsic intrusions in the Emeishan large igneous province[J]. *Geochimica et Cosmochimica Acta*, 75(5): 1374–1394.
- Zhong Hong, Xu Guiwen, Zhu Weiguang, Hu Ruizhong, He Defeng. 2009. Petrogenesis of the Taihe granites in the Emeishan large igneous province and its tectonic implications [J]. *Bulletin of Mineralogy, Petrology and Geochemistry*, 28(2): 99–110 (in Chinese with English abstract).
- Zhong Hong, Zhu Weiguang, Chu Zhuyin, He Defeng, Song Xieyan. 2007. SHRIMP U–Pb zircon geochronology, geochemistry, and Nd–Sr isotopic study of contrasting granites in the Emeishan large igneous province, SW China[J]. *Chemical Geology*, 236: 112–133.
- Zhong Hong, Zhu Weiguang, Hu Ruizhong, Xie Liewen, He Defeng, Liu Feng, Chu Zhuyin. 2009. Zircon U–Pb age and Sr–Nd–Hf isotope geochemistry of the Panzhihua A-type syenitic intrusion in the Emeishan large igneous province, southwest China and implications for growth of juvenile crust[J]. *Lithos*, 110(1/4): 109–128.
- Zhong Yuting, He Bin, Mundil R, Xu Yigang. 2014. CA-TIMS zircon U–Pb dating of felsic ignimbrite from the Binchuan section: Implications for the termination age of Emeishan large igneous province[J]. *Lithos*, 204: 14–19.
- Zhou Hongying, Li Huimin. 2011. U–Pb isotope dating technique and potential prospects for applying in geology[J]. *Geological Survey and Research*, 34(1): 63–70 (in Chinese with English abstract).
- Zhou Meifu, Arndt N T, Malpas J, Wang Christina Yan, Kennedy A K. 2008. Two magma series and associated ore deposit types in the Permian Emeishan large igneous province, SW China[J]. *Lithos*, 103(3/4): 352–368.
- Zhou Meifu, Malpas J, Song Xieyan, Robinson P T, Sun Min, Kennedy A K, Lesher C M, Keays R R. 2002. A temporal link between the Emeishan large igneous province (SW China) and the end-Guadalupian mass extinction[J]. *Earth and Planetary Science Letters*, 196(3/4): 113–122.
- Zhou Meifu, Robinson P T, Lesher C M, Keays R R, Zhang Chengjiang, Malpas J. 2005. Geochemistry, petrogenesis and metallogenesis of the Panzhihua gabbroic layered intrusion and associated Fe–Ti–V oxide deposits, Sichuan Province, SW China[J]. *Journal of Petrology*, 46(11): 2253–2280.
- Zhu Jiang, Zhang Zhaochong. 2013. The link between large igneous provinces and the two mass extinctions in Permian: Review of

- recent progress[J]. Geological Review, 59(1): 137–148(in Chinese with English abstract).
- Zhu Mingjin, Nie Aiguo, Tian Yazhou, Wang Xinsong, Sun Jun. 2019. Jurassic granitoid dike in Luodian, Guizhou Province: Discovery and geological significance[J]. Acta Geochimica, 38(1): 159–172.
- Zhu Mingjin, Tian Yazhou, Nie Aiguo, Zhang Heng, Yang Huashen. 2018. Petrogeochemistry, zircon SHRIMP U-Pb geochronology of mafic dykes in South Guizhou and their geological implication[J]. Earth Science, 43(4): 1333–1349 (in Chinese with English abstract).
- Zindler A, Hart S R. 1986. Chemical geodynamics[J]. Annual Review of Earth and Planetary Sciences, (14): 493–571.

附中文参考文献

- 崔金栋. 2013. 黔中隆起及周缘构造演化的沉积响应[D]. 长沙: 中南大学.
- 邓奇, 汪正江, 任光明, 崔晓庄, 曹华文, 宁括步, 任飞. 2020. 扬子地块西北缘~2.09 Ga 和~1.76 Ga 花岗质岩石: Columbia 超大陆聚合-裂解的岩浆记录[J]. 地球科学, 45(9): 3295–3312.
- 贵州省地质矿产局. 1987. 贵州省区域地质志[M]. 北京: 地质出版社. 554–596.
- 韩伟. 2010. 紫云—罗甸—南丹裂陷带的构造演化及地质意义[D]. 西安: 西北大学.
- 韩伟, 罗金海, 樊俊雷, 曹远志, 张静艺. 2009. 贵州罗甸晚二叠世辉绿岩及其区域构造意义[J]. 地质论评, 55(6): 795–803.
- 黄勇, 陈能松, 戴传固, 韩颖平, 白龙, 邓小杰. 2017. 罗甸玉矿区基性岩床内中性岩的锆石 U-Pb 定年及意义[J]. 贵州地质, 34(2): 90–96.
- 郝家树, 张国祥, 韩颖平, 邓小杰, 蒋艳霞, 强希润. 2014. 贵州南部中性岩浆岩的发现及其意义[J]. 贵州地质, 36(1): 52–55.
- 姜寒冰, 姜常义, 钱壮志, 朱士飞, 张蓬勃, 唐冬梅. 2009. 云南峨眉山高铁和低钛玄武岩的岩石成因[J]. 岩石学报, 25(5): 1117–1134.
- 罗震宇, 徐义刚, 何斌, 石玉若, 黄小龙. 2006. 论攀西猫猫沟霞石正长岩与峨眉山大火成岩省的成因联系: 年代学和岩石地球化学证据[J]. 科学通报, 51(15): 1802–1810.
- 李宏博, 张招崇, 吕林素. 2010. 峨眉山大火成岩省基性墙群几何学研究及对地幔柱中心的指示意义[J]. 岩石学报, 26(10): 3143–3152.
- 李宏博, 张招崇, 李永生. 2015. 云南富民晚二叠世中—基性岩年代学、地球化学特征: 对峨眉山大火成岩省岩浆作用过程的指示意义[J]. 地质学报, 89(1): 18–36.
- 李献华. 1996. 扬子南缘沉积岩的 Nd 同位素演化及其大地构造意义[J]. 岩石学报, 12(3): 359–369.
- 李献华, 李寄, 刘颖, 陈多福, 王一先, 赵振华. 1999. 华夏古陆古元古代变质火山岩的地球化学特征及其构造意义[J]. 岩石学报, 15(3): 364–371.
- 骆文娟, 张招崇, 侯通, 王萌. 2011. 攀西茨达复式岩体年代学和地球化学: 对峨眉山地幔柱活动时间的约束[J]. 岩石学报, 27(10): 2947–2962.
- 邵辉, 徐义刚, 何斌, 黄小龙, 罗震宇. 2007. 峨眉山大火成岩省晚期酸性火山岩的岩石地球化学特征[J]. 矿物岩石地球化学通报, 26(4): 350–358.
- 吴根耀. 2000. 华南的格林威尔造山带及其坍塌: 在罗迪尼亞超大陆演化中的意义[J]. 大地构造与成矿学, 24(2): 112–123.
- 汪正江. 2008. 黔东地区新元古代裂谷盆地演化及地层划分对比研究[D]. 北京: 中国地质科学院.
- 王登红. 2001. 地幔柱的概念、分类、演化与大规模成矿——对中国西南部的探讨[J]. 地学前缘, 8(3): 67–2.
- 王登红, 李建康, 刘峰, 陈振宇. 2004. 地幔柱研究中几个问题的探索及其找矿意义[J]. 地球学报, 25(5): 489–494.
- 王尚彦, 张慧, 彭成龙, 陈明华, 石磊, 张权莉, 王红梅, 王天华, 王纯厚, 胡仁发. 2005. 贵州西部古—中生代地层及裂陷槽盆的演化[M]. 北京: 地质出版社, 1–143.
- 王尚彦, 张慧, 王天华, 王纯厚, 彭成龙, 胡仁发, 陈明华, 石磊. 2006. 黔西水城—紫云地区晚古生代裂陷槽盆充填和演化[J]. 地质通报, 25(3): 402–407.
- 徐义刚, 何斌, 黄小龙, 罗震宇, 朱丹, 马金龙, 邵辉. 2007. 地幔柱大辩论及如何验证地幔柱假说[J]. 地学前缘, 14(2): 1–9.
- 徐义刚, 何斌, 罗震宇, 刘海泉. 2013. 我国大火成岩省和地幔柱研究进展与展望[J]. 矿物岩石地球化学通报, 32(1): 25–39.
- 杨明桂, 余忠珍, 徐梅桂, 唐维新, 王光辉, 胡青华. 2015. 晋宁期华南洋的构造格局[C] //第十三届华东六省一市地学科技论坛, 江西: 江西省地质学会, 1–17.
- 张招崇, 王福生, 范蔚茗, 邓海琳, 徐义刚, 许继峰, 王岳军. 2001. 峨眉山玄武岩研究中的一些问题的讨论[J]. 岩石矿物学杂志, 20(3): 239–246.
- 张招崇, 王福生, 郝艳丽. 2005. 峨眉山大火成岩省中的苦橄岩: 地幔柱活动证据[J]. 矿物岩石地球化学通报, 24(1): 17–22.
- 钟宏, 徐桂文, 朱维光, 胡瑞忠, 何德锋. 2009. 峨眉山大火成岩省太和花岗岩的成因及构造意义[J]. 矿物岩石地球化学通报, 2009(2): 99–110.
- 赵正, 漆亮, 黄智龙, 严再飞, 许成. 2012. 攀西裂谷南段鸡街碱性超基性岩微量元素和 Sr-Nd 同位素地球化学及其成因探讨[J]. 岩石学报, (6): 1915–1927.
- 祝明金, 田亚洲, 聂爱国, 张恒, 杨华燊. 2018. 黔南基性岩墙岩石地球化学、SHRIMP 锆石 U-Pb 年代学及地质意义[J]. 地球科学——中国地质大学学报, 43(4): 1333–1349.
- 曾广乾, 何良伦, 杨坤光. 2014. 黔西普安辉绿岩的年代学、地球化学特征及其地质意义[J]. 矿物岩石, 34(4): 61–70.
- 张晓静, 肖加飞. 2014. 桂西北玉凤、巴马晚二叠世辉绿岩年代学、地球化学特征及成因研究[J]. 矿物岩石地球化学通报, 33(2): 163–176.
- 周红英, 李惠民. 2011. U-Pb 同位素定年技术及其地质应用潜力[J]. 地质调查与研究, 34(1): 63–70.
- 章清文, 朱丹, 许英奎. 2015. 大陆地壳熔融和酸性岩浆起源的热源问题[J]. 矿物学报, 35(1): 44–50.
- 朱江, 张招崇. 2013. 大火成岩省与二叠纪两次生物灭绝关系研究进展[J]. 地质论评, 59(1): 137–148.